



American Society of Hematology  
2021 L Street NW, Suite 900,  
Washington, DC 20036  
Phone: 202-776-0544 | Fax 202-776-0545  
editorial@hematology.org

## **Plasma cell derived mtDAMPs activate macrophage STING pathway which promotes myeloma progression.**

Tracking no: BLD-2022-018711R1

Aisha Jibril (University of East Anglia, United Kingdom) Charlotte Hellmich (Norfolk and Norwich University Hospital, United Kingdom) Edyta Wojtowicz (Earlham Institute/University of East Anglia, United Kingdom) Katherine Hampton (The University of East Anglia, United Kingdom) Rebecca Maynard (The University of East Anglia, United Kingdom) Ravindu De Silva (Norfolk and Norwich University Hospital, United Kingdom) Dominic Fowler-Shorten (University of East Anglia, United Kingdom) Jayna Mistry (The Jackson Laboratory, United States) Jamie Moore (The University of East Anglia, United Kingdom) Kristian Bowles (University of East Anglia, United Kingdom) Stuart Rushworth (The University of East Anglia, United Kingdom)

### **Abstract:**

Mitochondrial damage-associated molecular patterns (mtDAMPs) include proteins, lipids, metabolites and DNA and have various context specific immunoregulatory functions. Cell-free mitochondrial DNA (mtDNA) is recognised via pattern recognition receptors and is a potent activator of the innate immune system. Cell-free mtDNA is elevated in the circulation of trauma and cancer patients, however the functional consequences of elevated mtDNA are largely undefined. Multiple myeloma (MM) relies upon cellular interactions within the bone marrow (BM) microenvironment for survival and progression. Here, using in-vivo models, we describe the role of MM cell derived mtDAMPs in the pro-tumoral BM microenvironment, and the mechanism and functional consequence of mtDAMPs in myeloma disease progression. Initially, we identified elevated levels of mtDNA in the peripheral blood serum of MM patients compared to healthy controls. Using the MM1S cells engrafted into NSG mice we established that elevated mtDNA was derived from MM cells. We further show that BM macrophages sense and respond to mtDAMPs through the STING pathway and inhibition of this pathway reduces MM tumor-burden in the KaLwRij-5TGM1 mouse model. Moreover, we found that MM derived mtDAMPs induced upregulation of chemokine signatures in BM macrophages and inhibition of this signature resulted in egress of MM cells from the BM. Here, we demonstrate that malignant plasma cells release mtDNA, a form of mtDAMPs, into the myeloma BM microenvironment, which in turn activates macrophages via STING signalling. We establish the functional role of these mtDAMP-activated macrophages in promoting disease progression and retaining MM cells in the pro-tumoral BM microenvironment.

**Conflict of interest:** No COI declared

**COI notes:**

**Preprint server:** No;

**Author contributions and disclosures:** A.J., C.H., K.M.B, and S.A.R designed the research; J.A.M., K.H., J.J.M, C.H., R.M., E.E.W. and A.J. performed the research; A.J., S.A.R. and C.H. carried out in vivo work; K.M.B., and C.H., provided essential reagents and knowledge. A.J., C.H., K.M.B., and S.A.R. wrote the paper.

**Non-author contributions and disclosures:** No;

**Agreement to Share Publication-Related Data and Data Sharing Statement:** All relevant data are included in the manuscript and the supporting information files. The data generated in this study are provided upon request from the corresponding authors

**Clinical trial registration information (if any):**

Plasma cell derived mtDAMPs activate macrophage STING pathway which promotes myeloma progression.

Aisha Jibril<sup>1\*</sup>, Charlotte Hellmich<sup>1,2\*</sup>, Edyta E Wojtowicz<sup>1,3</sup>, Katherine Hampton<sup>1</sup>, Rebecca Maynard<sup>1</sup>, Ravindu De Silva<sup>1,2</sup>, Dominic J Fowler-Shorten<sup>1</sup>, Jayna J Mistry<sup>1</sup>, Jamie A Moore<sup>1</sup>, Kristian M Bowles<sup>1,3\*\*</sup> and Stuart A Rushworth<sup>1\*\*</sup>

<sup>1</sup> Norwich Medical School, University of East Anglia, Norwich Research Park, Norwich, NR4 7UQ, United Kingdom.

<sup>2</sup> Department of Haematology, Norfolk and Norwich University Hospitals NHS Trust, Colney Lane, Norwich, NR4 7UY, United Kingdom

<sup>3</sup> Earlham Institute, Norwich Research Park, Norwich, NR4 7UH, United Kingdom

\* Denotes joint first author

\*\*Denotes joint corresponding author

**Running Title:** MM mtDAMPs regulate the tumor microenvironment

The authors declare no competing interests

Corresponding authors: Dr Stuart Rushworth and Prof Kristian Bowles, Department of Molecular Haematology, Norwich Medical School, Norwich Research Park, Norwich, NR4 7UQ, United Kingdom. email: [s.rushworth@uea.ac.uk](mailto:s.rushworth@uea.ac.uk) and [k.bowles@uea.ac.uk](mailto:k.bowles@uea.ac.uk)

Word count for text: 3978

Word count for abstract: 249

Figure count: 5

Table count: 1

Reference count: 43

**Key Points:**

- Cell-free mitochondrial DNA is elevated in the peripheral blood and bone marrow of myeloma patients compared to healthy controls.
- Myeloma derived mtDNA remodels the BM microenvironment, through its effect of STING activation in myeloma associated macrophages.

**Abstract**

Mitochondrial damage-associated molecular patterns (mtDAMPs) include proteins, lipids, metabolites and DNA and have various context specific immunoregulatory functions. Cell-free mitochondrial DNA (mtDNA) is recognised via pattern recognition receptors and is a potent activator of the innate immune system. Cell-free mtDNA is elevated in the circulation of trauma and cancer patients, however the functional consequences of elevated mtDNA are largely undefined. Multiple myeloma (MM) relies upon cellular interactions within the bone marrow (BM) microenvironment for survival and progression. Here, using in-vivo models, we describe the role of MM cell derived mtDAMPs in the pro-tumoral BM microenvironment, and the mechanism and functional consequence of mtDAMPs in myeloma disease progression. Initially, we identified elevated levels of mtDNA in the peripheral blood serum of MM patients compared to healthy controls. Using the MM1S cells engrafted into NSG mice we established that elevated mtDNA was derived from MM cells. We further show that BM macrophages sense and respond to mtDAMPs through the STING pathway and inhibition of this pathway reduces MM tumor-burden in the KaLwRij-5TGM1 mouse model. Moreover, we found that MM derived mtDAMPs induced upregulation of chemokine signatures in BM macrophages and inhibition of this signature resulted in egress of MM cells from the BM. Here, we demonstrate that malignant plasma cells release mtDNA, a form of mtDAMPs, into the myeloma BM microenvironment, which in turn activates macrophages via STING signalling. We establish the functional role of these mtDAMP-activated macrophages in promoting disease progression and retaining MM cells in the pro-tumoral BM microenvironment.

## Introduction

Despite significant advances made in the treatment of multiple myeloma (MM), relapse from chemo-refractory clones is inevitable, and most people diagnosed with MM will eventually die of the disease<sup>1-3</sup>. These observations are attributable, in part, to the highly immuno-protective and chemo-protective nature of the BM microenvironment, in which the malignant plasma cells proliferate and evolve. The BM microenvironment is a complex and highly organised tissue which physiologically supports the life-long production of blood cells from hematopoietic stem cells (HSC). HSCs reside in niches within the BM and are regulated through interactions with multiple cell types in the microenvironment, regulated by direct cell-cell contact, growth factors, cytokines and chemokines<sup>4-6</sup>. Macrophages are phagocytic immune cells present in most tissues, which exhibit plasticity and heterogeneity depending on their location. Within the BM, macrophages are split into several distinct populations with different functions, including regulating HSC maintenance and quiescence, supporting red cell development, and negatively regulating the HSC pool in response to infection<sup>5,7-9</sup>. In blood cancer, depletion of macrophages prevents engraftment of tumor cells in the BM. Moreover, tumor associated macrophages (TAMs) appear to be more broadly fundamentally involved in progression and metastasis, which across a range of cancers is linked to poorer clinical outcomes, in a diverse spectrum of tumor microenvironments<sup>10,11</sup>. In myeloma, increased numbers of TAMs have been described in the BM of MM patients with active disease<sup>12,13</sup>, and these cells exert a number of pro-tumoral functions including chemotherapy resistance, tumor retention in the BM, angiogenesis, proliferation and immunosuppression<sup>12-14</sup>. Collectively these studies show the protective effects of macrophages on myeloma, however, how and why macrophages maintain myeloma within the BM is not well understood.

Mitochondrial damage-associated patterns (mtDAMPs) include proteins, lipids, metabolites and DNA and have various context-specific immunoregulatory functions<sup>15,16</sup>. MtDAMPs have come into focus as mediators of inflammation, with mitochondrial DNA (mtDNA) being the most documented<sup>16,17</sup>. Cell-free mtDNA contains islands of unmethylated cytosine-guanine dinucleotide (CpG) motifs which are recognised via pattern recognition receptors and are potent activators of the innate immune system<sup>18</sup>. MtDNA has been identified as a potential biomarker for cancers due to its ease of detection in blood and non-invasive sample collection<sup>19</sup>.

Elevated levels of mtDNA in blood have been observed in many disease states from depression to prostate cancer, however, the majority of the literature on this has been essentially observational. In myeloma, studies have shown mtDNA copy number is elevated in the pre-symptomatic state monoclonal gammopathy of undetermined significance (MGUS) and MM patients<sup>20</sup>, but to date, no studies have reported the functional consequences of increased mtDNA in MM. Furthermore, mtDNA has been shown to activate the stimulator of interferon genes (STING) via cyclic GMP-AMP synthase (cGAS)<sup>21,22</sup>. The cGAS–STING signalling pathway is a key mediator of inflammation caused by infection, cellular stress or tissue damage. The cGAS–STING pathway detects and regulates the cellular response towards microbial and host-derived DNAs<sup>23</sup>.

In order to further elucidate the pro-tumoral cellular interactions between malignant plasma cells and the BM microenvironment here we present data which describes the role of MM cell derived mtDAMPs in the BM microenvironment, their role in STING pathway activation in macrophages and the mechanism and functional consequence of mtDAMPs on MM disease progression.

## **Materials and Methods**

### **Primary Tissue Collection**

Primary multiple myeloma samples were obtained from bone marrow aspirates from multiple myeloma patients at the Norfolk and Norwich University Hospital after informed consent and under the approval of the UK Health Research Authority and East of England Research Ethics Committee (IRAS project ID: 33753). In addition, CD34+ cells were isolated from human cord blood from patients undergoing elective caesarean sections and PB samples were collected from patients with myeloma or healthy controls following informed consent. Cell isolation was performed via density-gradient centrifugation of samples using Histopaque-1077 (Millipore Sigma). All cells were cultured in DMEM supplemented with 10% FBS and 1% Penicillin/Streptomycin and incubated at 37°C with 5% CO<sub>2</sub> humidity.

### **Animals**

Nonobese diabetic (NOD) severe combined immunodeficient (SCID) gamma mice (NOD. Cg-Prkdcscid Il2rgtm1Wjl/SzJ) and C57BL/KaLwRij were purchased from Jackson Laboratory (Bar Harbour, ME, USA). C57BL/6J and CBA mice were purchased from Charles River Laboratories (Massachusetts, United States). Mice were housed under specific pathogen-free conditions, in a containment level 3 disease modelling unit. All animal work was carried out in accordance with the Animal Scientific Procedures Act 1986 following UK Home Office Regulations. Mice of both genders were used in experiments and were between 6-12 weeks of age.

NSG mice were treated with 25mg/kg busulfan intraperitoneally every day for three days prior to the intravenous tail vein injection of  $2 \times 10^5$  MM1s cells. The cells were allowed to engraft over a period of 3 weeks. Blood samples were taken by tail vein bleed, the serum analysed by real-time qPCR to analyse presence of mtDNA. Engraftment was observed by flow cytometry through analysis of human CD38+ cells in the BM.

C57BL/KaLwRij mice were tail vein injected with  $1 \times 10^6$  5TGM1-GFP/luci cells. Throughout any experiment in vivo bioluminescence imaging (Bruker In Vivo Xtreme) was used to monitor tumor progression. Blood samples were taken by tail vein bleed

at various intervals for downstream analysis. At the end point BM was extracted for further analysis.

### **In Vivo STING inhibition Migration Assay**

C57BL/KaLwRij mice were engrafted with  $1 \times 10^6$  5TGM1<sup>(GFP+ Luci+)</sup> cells and engrafted for 34 days. On day 34, peripheral blood samples were taken prior to treatment with H-151 (750nmol) administered intraperitoneally, after 24 hours another peripheral blood sample was taken to be analysed by flow cytometry for 5TGM1<sup>(GFP+)</sup> presence.

### **In Vivo Macrophage Depletion**

C57BL/KaLwRij mice were engrafted with  $1 \times 10^6$  murine 5TGM1<sup>(GFP+ Luci+)</sup> cells via i.v. injection. 13 days post-engraftment mice were intraperitoneally injected with 150µl of either control or clodronate-loaded liposomes (Clophosome®-A, Stratech, UK). 24 hours later, the mice were sacrificed, and the bone marrow and peripheral blood were isolated for analysis. Flow cytometry was used to analyse BM macrophage population (GR1-, CD115<sup>LO/INT</sup>, F4/80+) and 5TGM1<sup>(GFP+)</sup> content in the peripheral blood and bone marrow to assess 5TGM1 cell homing.

### **Statistics**

GraphPad Prism, version 9 for macOS (GraphPad Software) was used to compare statistical significance. Due to variability in the data, statistical comparison of in vivo work was performed without assumption of normal distribution. Therefore, non-parametric statistical tests were used. For statistical comparison of groups of two a Mann-Whitney U test was performed. A Kruskal-Wallis test followed by Dunn's multiple comparisons was carried out for the comparison of groups larger than two. The Wilcoxon matched pairs signed rank test was used for statistical analysis between matched samples. Differences amongst groups were considered significant when the *P* value was less than 0.05.

### **Study approval**

All animal work used in this study were carried out in accordance with regulations set by the UK Home Office and the Animal Scientific Procedures Act 1986. Non-malignant and malignant haematopoietic cells were collected at the Norfolk and

Norwich University Hospital. Studies were performed following approval from the United Kingdom Health Research Authority research ethics committee (ref 07/H0310/146).

## Results

### **Cell-free mitochondrial DNA is elevated in multiple myeloma.**

To initially identify and quantify mtDAMPs in MM we used cell-free mtDNA as a surrogate marker. BM and peripheral blood (PB) samples were collected from newly diagnosed MM patients (Table 1). PB samples were also collected from healthy controls. Cell-free serum was obtained as described in Figure 1A, and qPCR was used to detect and quantify the presence of mtDNA. Figure 1B shows mtDNA to be elevated in the PB serum of patients with MM compared to controls (Figure 1B), with no significant change in genomic (gDNA) levels between MM and healthy controls (Figure 1C). Furthermore, comparing mtDNA levels in BM serum to matched PB serum from patients with MM, showed a significant increase in cell-free mtDNA in the BM (Figure 1D), suggesting that the majority of cell-free mtDNA associated with MM is maintained within the BM microenvironment. To further determine if MM was associated with increased cell-free mtDNA we analysed culture media from three control cell types (human CD34+ cells, B cells and monocytes), primary CD138+ plasma cells and immortalised MM cell lines (Figure 1E). CD34+ cells, B cells (CD19+) and monocytes (CD14+) cells were used as controls, as the frequency of plasma cells in healthy individuals is extremely low, and it is therefore difficult to isolate sufficient plasma cells for a direct comparison in these experiments. Results confirm that cell-free mtDNA is associated with myeloma (Figure 1F, Supplementary Figure 1A-B).). These data show that cell-free mtDNA is elevated in MM.

### **Increased mitochondrial DNA in MM originates from the malignant plasma cells**

To ascertain the origin of cell-free mtDNA detected at increased levels in the serum and BM of patients with MM we next studied the blood of immunocompromised NSG mice engrafted with the immortalised human MM cell line MM1S. PB samples were taken once a week over the course of 3 weeks, and serum was extracted for mtDNA analysis (Figures 2A and B). The serum was analysed by qPCR for human and murine mitochondrial DNA. Fold change in mtDNA at day 7 was used as a baseline to assess mtDNA change over the 21 days. We observe no change in the levels of murine mtDNA in both control and engrafted mice over time (Figure 2C). However, human mtDNA levels first became detectable on day 14 and increased further by day 21 in MM1s engrafted mice. The human origin of the mtDNA was confirmed

further with a second human mitochondrial target (Supplementary Figure 2A). We detected no human mtDNA detected in control mice at the same time points. Engraftment of the MM1S cells in mice was confirmed by measuring the percentage of human CD38+ cells in the BM by flow cytometry (Figure 2D). To confirm the MM1S-NSG model results, we repeated the experiment described and engrafted NSG mice with MM1S cells. For this experiment, we analysed the levels of mtDNA in both the PB and BM serum after 21 days post injection of MM1s cells. We observed elevated levels of human mtDNA in the PB serum which was significantly enhanced in the BM serum (Figure 2E). Together with the data from Figure 1D this shows that BM serum in myeloma patients and MM mouse models has increased levels of myeloma derived mtDNA compared to PB serum.

Finally, to exclude the possibility that these data represented a cross species or an unexpected NSG model phenomena we used a isogenic murine model of MM. In similar experiments using the KaLwRij-5TGM1 isogenic mouse model of myeloma we confirmed the presence of elevated levels of mtDNA in the PB of animals with MM (Figure 2F-G). To determine if the increase in mtDNA is specific to myeloma or also occurs in other haematological malignancies, we used our established mouse model of acute myeloid leukaemia<sup>10</sup>. The BM serum of mice engrafted with MN1 cells did not show an increase in mtDNA (Supplementary Figure 2B-C). Together, these data suggest that malignant plasma cells are the source of increased levels of mtDNA in MM, which originate in the tumor microenvironment and egresses into the circulation.

### **MM induces STING-mediated activation of macrophages via mtDAMPs**

To address the functional consequence of myeloma derived mtDNA on the BM microenvironment we performed studies on macrophages from the tumor microenvironment. We and others have recently shown that macrophages and effector cells react to mtDAMPs via the STING pathway, in the contexts of inflammation<sup>22</sup>, ischemia and acute myeloid leukemia<sup>10</sup>. Accordingly, we analysed a panel of genes associated with STING pathway activation, in macrophages isolated from 5TGM1<sup>(GFP+ LUCI+)</sup> engrafted KaLwRij mice (Figure 3A). Engraftment of 5TGM1 in the KaLwRij mice was determined by GFP expressing cells in the BM (Figure 3B). Sorting strategy for the BM macrophages is shown in Figure 3C and as previously

described<sup>10</sup>. RT-qPCR showed increased expression of *GBP2*, *IFIT3*, and *IRF7* in BM macrophages FACS purified from 5TGM1 engrafted mice (Figure 3D). To determine if STING pathway activation in macrophages was directly related to secreted components from MM, we cultured BMDM from KaLwRij mice with 5TGM1 conditioned media that had undergone centrifugation to remove cells and large extracellular vesicles (EVs) and further filtered through a 100 kDa ultra-centrifugal filter to remove small EVs and any other remaining large proteins (Figure 3E). These centrifugation steps to remove large and small EVs were included as others have shown that whole functional mitochondria can be packaged in EV and transferred between cells<sup>24,25</sup>. Removal of the EVs therefore allowed us to purely focus on the effect of cell free mtDNA. Results show that STING-pathway genes were upregulated in BMDM treated with conditioned media from 5TGM1 (Figure 3F). This suggested that MM cells release small cell-free molecules that trigger STING activation in macrophages.

To determine whether this was a specific mtDNA or a broader mtDAMP response, we treated BMDMs with mtDAMPs obtained from mouse liver or CpG ODN 1826 (a molecular mimic of mtDNA) and looked at gene expression of STING activation genes. The purity of mtDAMPs used was confirmed using PCR for mtDNA and genomic DNA, which showed that only mtDNA could be detected in the mtDAMPs used (Supplementary Figure 3A). Whilst mtDAMP treatment resulted in the upregulation of all STING genes (Figure 3G), CpG treatment failed to fully activate the STING-related genes with only *Irf7* being significantly upregulated (Figure 3H). To determine if raised levels of mtDNA in patients with myeloma also correlates with changes in STING genes, monocytes were isolated from the peripheral blood of patients newly diagnosed with myeloma and healthy controls. The results show that STING genes were upregulated in monocytes collected from the peripheral blood of myeloma patients compared to controls (Supplementary Figure 3B). Finally, to confirm that this response was mediated through STING we used the STING inhibitor H-151 to block the mtDAMP-induced STING activation pathway. Figure 3I shows that treatment with H-151 inhibits mtDAMP-induced STING activation genes in BMDM. The data suggest that mtDAMPs released from myeloma cells induce a STING response in BM macrophages.

### **MM progression is attenuated by STING inhibition**

To understand the tumor specific functional consequences of STING activation by MM-derived mtDAMPs in the microenvironment, KaLwRij mice were engrafted with 5TGM1<sup>(GFP+Luci+)</sup> cells and the tumor was allowed to establish for 19 days, before 1-week of treatment with STING inhibitor H-151 (Figure 4A). The animals were imaged before and after treatment, and bioluminescent images show reduced tumor progression in the H-151 treated group from day 19 to day 27, despite similar engraftment in the two treatment groups on day 19 (Figure 4B and C and Supplementary Figure 4A and B). The animals were then sacrificed and tumor volume was measured by flow cytometry for GFP+ cells. When compared with control 5TGM1 engrafted animals, H-151 treated animals had reduced tumor volume (Figure 4D). BM was isolated from sacrificed animals and BM macrophages were FACS purified and analysed for *GBP2*, *IFIT3* and *IRF7* gene expression. When compared with control animals, BM macrophages from H-151 treated animals had trend towards decreased expression of STING markers, *GBP2*, *IRF7* and *IFIT3* (Figure 4E). Flow cytometry was also used to analyse the BM resident and infiltrating macrophage cell populations in the tumor microenvironment. We found that there were no significant differences in the size of these populations, nor the polarisation of M1 (CD86+) or M2 (CD206+) macrophages with STING inhibition (Figure 4F and G). Finally, 5TGM1 cells were treated with 10µM of H-151 for 24 hours and cell survival was then measured using a CellTiter Glo assay (Supplementary Figure 4C). The results show that H-151 has no direct effect on 5TGM1 survival.

### **MM-derived mtDAMPs Induce a migratory signature in BM macrophages**

To investigate the secretome changes in macrophages exposed to MM-derived mtDAMPs, we treated BMDMs with myeloma-derived mtDAMPs and assayed the cell supernatant using a Proteome Profiler Mouse Cytokine Array (Figure 5A). As predicted, we detected an upregulation in several cytokines including those associated with inflammation and STING pathway activation. However, in addition we observed a cluster of chemoattractant cytokines (CCL5, CXCL2 and CXCL10) that were also upregulated by mtDAMPs treated macrophages (Figure 5B). MM is primarily a BM disease with clonal plasma cells rarely detected in the PB at leukemic levels, reflected by the clinical observation that plasma cell leukemia represents <1% of all cases of MM<sup>26</sup>. Therefore, we hypothesised a role for MM-derived mtDAMPs

in promoting the retention of malignant plasma cells in the BM via activation of the STING pathway in macrophages. To address this, we first determined *in vivo* if these chemokines were upregulated in FACS-purified BM macrophages from 5TGM1 engrafted KaLwRij mice and whether this upregulation could be inhibited by H-151 (Figure 5C). When compared to control BM macrophages from KaLwRij animals, macrophages from 5TGM1 engrafted animals had increased *CCL5*, *CXCL2* and *CXCL10* mRNA expression. Moreover, STING inhibition significantly reduced the expression of *CXCL2* and *CCL5* (Figure 5D). Next, we used an *in vitro* migration assay in which conditioned media from BMDM were treated with mtDAMPs with and without STING inhibition with H-151. Results show that conditioned media from mtDAMP treated macrophages increased the migration of 5TGM1 cells, whereas when STING signalling was inhibited cell migration was reduced (Figure 5E). Inhibitors for CCL5 (anti-CCL5 ab), CXCL10-CXCR3 (AMG487) and CXCL2-CXCR2 (SB225002) were used to determine the role of each pathway in the retention of MM. Inhibition of CCL5 significantly reduced mtDAMP induced migration (Supplementary Figure 5A). Moreover, STING inhibition in 5TGM1 engrafted KaLwRij mice resulted in an increased frequency of 5TGM1 cells in the BM (Figure 5F). Finally, to establish the role of macrophages in the retention of myeloma in the BM marrow we used clodronate liposomes to deplete macrophages in the 5TGM1-KaLwRij engrafted model and then assess myeloma egress from the BM (Supplementary Figure 5B). The frequency of macrophages in the BM was reduced in clodronate treated animals (Supplementary Figure 5C). When compared to control liposome treated KaLwRij animals from 5TGM1 engrafted animals, clodronate liposome treatment showed increase levels of 5TGM1 cells in the PB and reduced tumor volume in the BM (Supplementary Figure 5D). Together, these data show that myeloma cells release mtDAMPs into the BM which activate resident macrophages to produce a chemotaxis signature resulting in myeloma BM retention.

## Discussion

MM represents a spectrum of genetically, molecularly and phenotypically incurable tumors which evolve and progress over time<sup>27</sup>. Even at early and asymptomatic stages of the disease, genetic and molecular diversity<sup>28</sup> and compromised immune microenvironment<sup>29</sup> can be identified. Furthermore, in relapse, there is an accumulation of additional genetic mutations, which activate oncogenic pathways and impact drug sensitivity<sup>30</sup>. Despite these observations demonstrating MM to be a set of highly genetically diverse<sup>31</sup>, molecularly distinct<sup>32</sup>, clinically varied<sup>33</sup>, and clonally unstable<sup>34</sup> disease entities, almost without exception all MM tumor subtypes, originate, proliferate and relapse within the BM microenvironment. This observation of a shared microenvironmental dependency for such a heterogeneous spectrum of disease implies a fundamental role for the non-malignant cells of the BM niche in MM pathophysiology and evolution. The commonality of this observation also leads to speculation that novel therapeutic strategies targeting the tumor-microenvironment interactions may have broad clinical efficacy despite such broad molecular and cellular diversity in these cancer subtypes.

Macrophages play a fundamental role in normal BM homeostasis. Moreover, in the tumor microenvironment interaction of the macrophages, tumor cells and stromal cells enables and sustains most of the hallmarks of cancer<sup>35</sup>. In MM, macrophages are abundant and have been shown to impact the initiation and progression the disease<sup>36</sup>, via a number of mechanisms of action including homing of malignant cells to BM, plasma cell proliferation, drug resistance, neovascularisation and immunosuppression<sup>37</sup>. Specifically, invasion of tumor supporting macrophages has been shown to correlate with low survival in patients with MM<sup>38</sup>. Here, we identified that STING-mediated activation of BM macrophages enhances MM progression by secreting migratory chemokines which retain MM in the protective BM. Other studies have shown that in the 5TGM1-KaLwRij model depletion of macrophages, using clodronate liposomes, before injection of 5TGM1 slows MM engraftment<sup>38</sup>. Moreover, they show that clodronate treatment decreases *CXCL12* expression in BM cells suggesting that this treatment is inhibiting homing of MM to the BM<sup>38</sup>. Another study by the same group shows that inhibition of CCL3/CCR1 interactions between MM and BM stromal cells causes egress of MM from the BM<sup>39</sup>. Collectively these

studies describe the importance of macrophages in the retention of MM in the BM, which supports survival, proliferation and chemotherapy resistance, and highlight the potential clinical value of drugs which interfere with these processes.

The presence of cell-free mtDNA has been found in the serum of patients with various cancer types<sup>40</sup>. Several groups have reported the diagnostic value of mtDNA in plasma, serum or whole blood as a biomarker of solid malignancies including lung, breast and testicular cancer<sup>19,41-43</sup> however, the understanding of the source of this mtDNA and its pathophysiological impact on cancer progression is less well established. In this study, we observed that mtDNA is elevated in cell-free serum samples from patients with MM. Moreover, through animal modelling, we showed that mtDNA detected in the serum originates from the tumor cell. We also observe increased cell-free mtDNA in myeloma patient PB serum compared to healthy controls, which is further elevated in the BM. Furthermore, we showed that the increased levels of cell-free mtDNA correlated with an upregulation of the STING-related genes in macrophages both in vivo and in vitro as well as in PB monocytes from patients with MM. As we could not exclude that the isolated mtDNA contained trace amounts of mtDAMPS, we used the mtDNA mimic, CPG ODN 1826 to determine if the response was specific to mtDNA or a broader mtDAMP response. Although, CPG ODN mimics cell-free mtDNA the concentration of CPG repeats is much higher than that contained in the mtDNA and therefore may have increased the functional response observed. Moreover, the use of CPG ODN 1826 at the concentrations used may not represent the physiological response observed in-vivo. However, using mtDMAPS also has its limitations as it is unclear which component Mitochondrial damage-associated molecular patterns (mtDAMPs) include proteins, lipids, metabolites and DNA and have various context specific immunoregulatory functions. Cell-free mitochondrial DNA (mtDNA) is recognised via pattern recognition receptors and is a potent activator of the innate immune system. Cell-free mtDNA is elevated in the circulation of trauma and cancer patients, however the functional consequences of elevated mtDNA are largely undefined. Multiple myeloma (MM) relies upon cellular interactions within the bone marrow (BM) microenvironment for survival and progression. Here, using in-vivo models, we describe the role of MM cell derived mtDAMPs in the pro-tumoral BM microenvironment, and the mechanism and functional consequence of mtDAMPs in myeloma disease progression. Initially, we

identified elevated levels of mtDNA in the peripheral blood serum of MM patients compared to healthy controls. Using the MM1S cells engrafted into NSG mice we established that elevated mtDNA was derived from MM cells. We further show that BM macrophages sense and respond to mtDAMPs through the STING pathway and inhibition of this pathway reduces MM tumor-burden in the KaLwRij-5TGM1 mouse model. Moreover, we found that MM derived mtDAMPs induced upregulation of chemokine signatures in BM macrophages and inhibition of this signature resulted in egress of MM cells from the BM. Here, we demonstrate that malignant plasma cells release mtDNA, a form of mtDAMPs, into the myeloma BM microenvironment, which in turn activates macrophages via STING signalling. We establish the functional role of these mtDAMP-activated macrophages in promoting disease progression and retaining MM cells in the pro-tumoral BM microenvironment. of the DAMP is responsible for the response observed and this would be particularly important to allow targeting of the mtDAMP response as a therapeutic intervention. Mechanistically, we show that myeloma-derived mtDAMPs rather than CPG ODN promoted pro-tumoral microenvironment remodelling by activating BM macrophage chemotaxis signatures through the activation of the STING pathway. Specifically, inhibition of mtDAMPs-induced STING activation promotes the egress of myeloma from the supporting BM microenvironment.

Targeting the cGAS/STING pathway has been shown to play an important role in many preclinical models of inflammation, chronic diseases, and cancer. In cancer, we and others have shown that STING activation can significantly extend survival in *in vivo* models of AML<sup>10,44</sup>. In this manuscript, describing the role of macrophages in the progression of MM, STING inhibition extends the survival of MM, which on the face of it appears contradictory to the results obtained in AML and other cancer models<sup>45</sup>. In some contexts, macrophages in the tumor microenvironment have been found to promote AML progression. Specifically, displacement of resident macrophages or invasion of tumor-supporting macrophages has been shown to correlate with low survival in patients with AML. In our previously published data on AML, LAP-dependent activation of STING increased the phagocytosis of AML cells<sup>10</sup>. In mouse melanoma cells and several other cell lines, the anthracycline drug doxorubicin, induced the activation of STING. Accordingly, the consequences of

STING activation/inhibition are not only tissue and cell specific but will also likely have different disease specific outcomes within the spectrum of BM disorders.

Macrophages play a number of important and often disease specific roles in the tumor microenvironment and given the association between high macrophage infiltration and poor survival in most cancers, identifying intra-tumoral macrophage specific therapeutic targets remains an important goal <sup>46</sup>. Here we identify a functional role for mtDNA in the myeloma BM microenvironment, through its effect of STING activation in myeloma-associated macrophages.

## **Acknowledgements**

The authors wish to thank the Norwich Research Park (NRP), The Rosetrees Trust, The Big C and the NHS. The authors also thank Dr Allyson Tyler and Dr Karen Ashurst from the Laboratory Medicine Department at the Norfolk and Norwich University Hospital (NNUH) for technical assistance. The authors also wish to thank Dr Rachel Stanley at the NRP Biorepository (UK) for supporting primary tissue collection as well as the team at the Disease Modelling Unit of the University of East Anglia for assistance with the in-vivo studies. E.E.W. is supported by a Sir Henry Wellcome Postdoctoral Fellowship (213731/Z/18/Z), J.A.M. was supported by Rosetrees Trust. C.H. is funded by Wellcome Trust Clinical Research Fellowship (220534/Z/20/Z). SAR is supported by the MRC project (MR/T02934X/1). The authors also acknowledge support from the BBSRC, part of UK Research and Innovation's Core Capability Grant BB/CCG1720/1, the National Capability (BBS/E/T/000PR9816) and the NNUH Charitable Fund.

## **Author Contribution**

A.J., C.H., K.M.B, and S.A.R designed the research; J.A.M., K.H., D.J.F-S., J.J.M, C.H., R.M., E.E.W. and A.J. performed the research; A.J., S.A.R. and C.H. carried out in vivo work; K.M.B., C.H. and R.DS., provided essential reagents and knowledge. A.J., C.H., K.M.B., and S.A.R. wrote the paper.

## **Declaration of interests**

The authors declare no competing interests

**Data Sharing Plan:** All relevant data are included in the manuscript and the supporting information files. The data generated in this study are provided upon request from the corresponding authors

## References

1. Hemminki K, Försti A, Hansson M. Incidence, mortality and survival in multiple myeloma compared to other hematopoietic neoplasms in Sweden up to year 2016. *Scientific Reports*. 2021;11(1):17272.
2. Mai EK, Haas E-M, Lücke S, et al. A systematic classification of death causes in multiple myeloma. *Blood Cancer Journal*. 2018;8(3):30.
3. Mohty M, Cavo M, Fink L, et al. Understanding mortality in multiple myeloma: Findings of a European retrospective chart review. *European Journal of Haematology*. 2019;103(2):107-115.
4. Nakahara F, Borger DK, Wei Q, et al. Engineering a haematopoietic stem cell niche by revitalizing mesenchymal stromal cells. *Nat Cell Biol*. 2019;21(5):560-567.
5. Pinho S, Frenette PS. Haematopoietic stem cell activity and interactions with the niche. *Nat Rev Mol Cell Biol*. 2019;20(5):303-320.
6. Saçma M, Pospiech J, Bogeska R, et al. Haematopoietic stem cells in perisinusoidal niches are protected from ageing. *Nat Cell Biol*. 2019;21(11):1309-1320.
7. Chow A, Lucas D, Hidalgo A, et al. Bone marrow CD169+ macrophages promote the retention of hematopoietic stem and progenitor cells in the mesenchymal stem cell niche. *J Exp Med*. 2011;208(2):261-271.
8. Winkler IG, Sims NA, Pettit AR, et al. Bone marrow macrophages maintain hematopoietic stem cell (HSC) niches and their depletion mobilizes HSCs. *Blood*. 2010;116(23):4815-4828.
9. Udagawa N, Takahashi N, Akatsu T, et al. Origin of osteoclasts: mature monocytes and macrophages are capable of differentiating into osteoclasts under a suitable microenvironment prepared by bone marrow-derived stromal cells. *Proc Natl Acad Sci U S A*. 1990;87(18):7260-7264.
10. Moore JA, Mistry JJ, Hellmich C, et al. LC3-associated phagocytosis in bone marrow macrophages suppresses acute myeloid leukemia progression through STING activation. *J Clin Invest*. 2022;132(5).
11. Cunha LD, Yang M, Carter R, et al. LC3-Associated Phagocytosis in Myeloid Cells Promotes Tumor Immune Tolerance. *Cell*. 2018;175(2):429-441.e416.
12. Zhang D, Huang J, Wang F, et al. BMI1 regulates multiple myeloma-associated macrophage's pro-myeloma functions. *Cell Death & Disease*. 2021;12(5):495.
13. Wang H, Hu WM, Xia ZJ, et al. High numbers of CD163+ tumor-associated macrophages correlate with poor prognosis in multiple myeloma patients receiving bortezomib-based regimens. *J Cancer*. 2019;10(14):3239-3245.
14. Sun J, Park C, Guenther N, et al. Tumor-associated macrophages in multiple myeloma: advances in biology and therapy. *Journal for ImmunoTherapy of Cancer*. 2022;10(4):e003975.
15. Wenceslau CF, McCarthy CG, Szasz T, Spitler K, Goulopoulou S, Webb RC. Mitochondrial damage-associated molecular patterns and vascular function. *Eur Heart J*. 2014;35(18):1172-1177.
16. Zhang Q, Raoof M, Chen Y, et al. Circulating mitochondrial DAMPs cause inflammatory responses to injury. *Nature*. 2010;464(7285):104-107.
17. Gong T, Liu L, Jiang W, Zhou R. DAMP-sensing receptors in sterile inflammation and inflammatory diseases. *Nature Reviews Immunology*. 2020;20(2):95-112.

18. Bellizzi D, D'Aquila P, Scafone T, et al. The control region of mitochondrial DNA shows an unusual CpG and non-CpG methylation pattern. *DNA Res.* 2013;20(6):537-547.
19. Afrifa J, Zhao T, You J. Circulating Mitochondria DNA, a non-invasive cancer diagnostic biomarker candidate. *Mitochondrion.* 2019;47.
20. Ruiz-Heredia Y, Ortiz-Ruiz A, Samur MK, et al. Pathogenetic and Prognostic Implications of Increased Mitochondrial Content in Multiple Myeloma. *Cancers (Basel).* 2021;13(13).
21. Bode C, Fox M, Tewary P, et al. Human plasmacytoid dendritic cells elicit a Type I Interferon response by sensing DNA via the cGAS-STING signaling pathway. *Eur J Immunol.* 2016;46(7):1615-1621.
22. Motwani M, Pesiridis S, Fitzgerald KA. DNA sensing by the cGAS-STING pathway in health and disease. *Nat Rev Genet.* 2019;20(11):657-674.
23. Decout A, Katz JD, Venkatraman S, Ablasser A. The cGAS-STING pathway as a therapeutic target in inflammatory diseases. *Nat Rev Immunol.* 2021;21(9):548-569.
24. Zhang Y, Tan J, Miao Y, Zhang Q. The effect of extracellular vesicles on the regulation of mitochondria under hypoxia. *Cell Death Dis.* 2021;12(4):358.
25. Amari L, Germain M. Mitochondrial Extracellular Vesicles - Origins and Roles. *Front Mol Neurosci.* 2021;14:767219.
26. Gundesen MT, Lund T, Moeller HEH, Abildgaard N. Plasma Cell Leukemia: Definition, Presentation, and Treatment. *Current Oncology Reports.* 2019;21(1):8.
27. Dutta AK, Alberge JB, Sklaventis-Pistofidis R, Lightbody ED, Getz G, Ghobrial IM. Single-cell profiling of tumour evolution in multiple myeloma - opportunities for precision medicine. *Nat Rev Clin Oncol.* 2022;19(4):223-236.
28. Bustoros M, Anand S, Sklaventis-Pistofidis R, et al. Genetic subtypes of smoldering multiple myeloma are associated with distinct pathogenic phenotypes and clinical outcomes. *Nature Communications.* 2022;13(1):3449.
29. Zavidij O, Haradhvala NJ, Mouhieddine TH, et al. Single-cell RNA sequencing reveals compromised immune microenvironment in precursor stages of multiple myeloma. *Nat Cancer.* 2020;1(5):493-506.
30. Vo JN, Wu Y-M, Mishler J, et al. The genetic heterogeneity and drug resistance mechanisms of relapsed refractory multiple myeloma. *Nature Communications.* 2022;13(1):3750.
31. Lohr Jens G, Stojanov P, Carter Scott L, et al. Widespread Genetic Heterogeneity in Multiple Myeloma: Implications for Targeted Therapy. *Cancer Cell.* 2014;25(1):91-101.
32. Ferguson ID, Patiño-Escobar B, Tuomivaara ST, et al. The surfaceome of multiple myeloma cells suggests potential immunotherapeutic strategies and protein markers of drug resistance. *Nature Communications.* 2022;13(1):4121.
33. Terpos E, Mikhael J, Hajek R, et al. Management of patients with multiple myeloma beyond the clinical-trial setting: understanding the balance between efficacy, safety and tolerability, and quality of life. *Blood Cancer J.* 2021;11(2):40.
34. Neuse CJ, Lomas OC, Schliemann C, et al. Genome instability in multiple myeloma. *Leukemia.* 2020;34(11):2887-2897.
35. Pittet MJ, Michielin O, Migliorini D. Clinical relevance of tumour-associated macrophages. *Nature Reviews Clinical Oncology.* 2022;19(6):402-421.
36. Zheng Y, Cai Z, Wang S, et al. Macrophages are an abundant component of myeloma microenvironment and protect myeloma cells from chemotherapy drug-induced apoptosis. *Blood.* 2009;114(17):3625-3628.

37. Opperman KS, Vandyke K, Psaltis PJ, Noll JE, Zannettino ACW. Macrophages in multiple myeloma: key roles and therapeutic strategies. *Cancer and Metastasis Reviews*. 2021;40(1):273-284.
38. Opperman KS, Vandyke K, Clark KC, et al. Clodronate-Liposome Mediated Macrophage Depletion Abrogates Multiple Myeloma Tumor Establishment In Vivo. *Neoplasia*. 2019;21(8):777-787.
39. Zeissig MN, Hewett DR, Panagopoulos V, et al. Expression of the chemokine receptor CCR1 promotes the dissemination of multiple myeloma plasma cells *in vivo*. *Haematologica*. 2021;106(12):3176-3187.
40. Grazioli S, Pugin J. Mitochondrial Damage-Associated Molecular Patterns: From Inflammatory Signaling to Human Diseases. *Front Immunol*. 2018;9:832.
41. Ellinger J, Albers P, Müller SC, von Ruecker A, Bastian PJ. Circulating mitochondrial DNA in the serum of patients with testicular germ cell cancer as a novel noninvasive diagnostic biomarker. *BJU Int*. 2009;104(1):48-52.
42. Mahmoud EH, Fawzy A, Ahmad OK, Ali AM. Plasma Circulating Cell-free Nuclear and Mitochondrial DNA as Potential Biomarkers in the Peripheral Blood of Breast Cancer Patients. *Asian Pac J Cancer Prev*. 2015;16(18):8299-8305.
43. Huang CY, Chen YM, Wu CH, et al. Circulating free mitochondrial DNA concentration and its association with erlotinib treatment in patients with adenocarcinoma of the lung. *Oncol Lett*. 2014;7(6):2180-2184.
44. Curran E, Chen X, Corrales L, et al. STING Pathway Activation Stimulates Potent Immunity against Acute Myeloid Leukemia. *Cell Rep*. 2016;15(11):2357-2366.
45. Wang Q, Bergholz JS, Ding L, et al. STING agonism reprograms tumor-associated macrophages and overcomes resistance to PARP inhibition in BRCA1-deficient models of breast cancer. *Nature Communications*. 2022;13(1):3022.
46. Poh AR, Ernst M. Targeting Macrophages in Cancer: From Bench to Bedside. *Front Oncol*. 2018;8:49.

Table 1

| <b>PATIENT NO.</b> | <b>AGE (YEARS)</b> | <b>SEX</b> | <b>DIAGNOSIS</b> |
|--------------------|--------------------|------------|------------------|
| <b>MM1</b>         | 59                 | F          | Myeloma (s)      |
| <b>MM2</b>         | 74                 | F          | Myeloma (s)      |
| <b>MM3</b>         | 72                 | F          | Myeloma (s)      |
| <b>MM4</b>         | 80                 | M          | Myeloma (a)      |
| <b>MM5</b>         | 37                 | M          | Myeloma (s)      |
| <b>MM6</b>         | 79                 | F          | Myeloma (s)      |
| <b>MM7</b>         | 69                 | M          | Myeloma (a)      |
| <b>MM8</b>         | 57                 | M          | Myeloma (s)      |
| <b>MM9</b>         | 66                 | F          | Myeloma (s)      |
| <b>MM10</b>        | 82                 | F          | Myeloma (a)      |
| <b>MM11</b>        | 74                 | M          | Myeloma (a)      |
| <b>MM12</b>        | 53                 | F          | Myeloma (s)      |
| <b>MM13</b>        | 64                 | M          | Myeloma (s)      |
| <b>MM14</b>        | 73                 | M          | Myeloma (s)      |
| <b>MM15</b>        | 75                 | F          | Myeloma (s)      |
| <b>MM16</b>        | 55                 | M          | Myeloma (s)      |
| <b>MM17</b>        | 75                 | F          | Myeloma (s)      |
| <b>MM18</b>        | 86                 | M          | Myeloma (a)      |
| <b>MM19</b>        | 83                 | F          | Myeloma (a)      |
| <b>MM20</b>        | 72                 | F          | Myeloma (s)      |
| <b>MM21</b>        | 62                 | M          | Myeloma (a)      |
| <b>MM22</b>        | 49                 | F          | Myeloma (a)      |
| <b>MM23</b>        | 80                 | F          | Myeloma (s)      |
| <b>MM24</b>        | 63                 | F          | Myeloma (s)      |
| <b>MM25</b>        | 66                 | F          | Myeloma (a)      |
| <b>MM26</b>        | 60                 | F          | Myeloma (a)      |

F, Female; M, Male; a, Asymptomatic; s, Symptomatic.

Table 1: Myeloma patient data. Samples MM1-MM11 were used for matched analysis of peripheral blood and bone marrow in Figure 1D. Samples MM12-MM19 were used for Figure 1B and C. Samples MM 20-26 were used for Supplementary Figure 2B.

## Figure Legends

**Figure 1. Cell-free mitochondrial DNA is elevated in myeloma.** (A) Schematic of the serum extraction process. DNA was extracted from patient peripheral blood (PB) serum and analysed via TaqMan qPCR to assess mitochondrial and genomic DNA (mtDNA and gDNA) content. (B) Fold change in serum mtDNA in healthy (n=9) vs myeloma patients (n=21). (C) Fold change in serum gDNA. (D) mtDNA changes from matched MM patient PB and BM serum (n=11). Data indicate mean  $\pm$ SD. Statistics are presented as Mann-Whitney U test. \*\*\*P < 0.001 (E) Schematic of the cell-free media extraction process. DNA was extracted from cell-free media extracted from cells in culture and analysed via TaqMan qPCR. (F) Fold change in mtDNA in the media of control CD34+ cells (n=6), MM patient-derived cells (n=6) and immortalised MM cell lines (n=4). Data indicate mean  $\pm$ SD. Statistics are presented as Wilcoxon test. \*\*P < 0.01.

**Figure 2. Mitochondrial DNA is released by MM cells.** (A and B) Schematic of experimental design. Human MM1s ( $2 \times 10^6$ ) were injected I.V into busulfan (25mg/kg) pre-treated NSG mice. Peripheral blood samples were taken via I.V tail vein bleed at 7- and 14-days post-engraftment. (C) Cell-free serum was extracted from peripheral blood via centrifugation, and DNA was extracted and analysed via qPCR for the presence of murine and human mtDNA, using human and mouse ND1 primers. (D) Percentage of human CD38+ cells in the bone marrow of control NSG mice (n=4) and NSG-MM1s mice (n=4). (E) In a separate experiment human MM1s ( $2 \times 10^6$ ) were injected I.V into busulfan (25mg/kg) pre-treated NSG mice. At 21 days peripheral blood and BM samples were taken and cell-free serum was taken, and DNA extracted and analysed via qPCR for mtDNA. (F-G)  $1 \times 10^6$  murine 5TGM1<sup>(GFP+Luci+)</sup> cells were injected into C57BL/KaLwRij mice, mice were sacrificed at 21 days and peripheral blood serum samples were extracted and analysed via qPCR for mtDNA. Data indicate mean  $\pm$ SD. Statistics are presented as Mann-Whitney U test. \*P < 0.05.

**Figure 3. MM induces STING-mediated activation of macrophages via mtDAMPs** (A) Schematic of experimental design. Murine 5TGM1 cells ( $1 \times 10^6$ ) were injected into KaLwRij mice. (B) At 28 days BM samples were taken and analysed for

5TGM1 engraftment by GFP+ cells. (C) BM macrophages were FACS purified (GR1-, F4/80+, CD115<sup>int</sup>) and RNA extracted for analysis by qRT-PCR. (D) Relative gene expression of *GBP2*, *IFIT3* and *IRF7* in FACS purified macrophages. (E) Large and small EV were removed from 5TGM1 conditioned media (CM) by centrifugation and filtering through a 100kDa Amicon Ultra-15 centrifugal filter. (F) BMDM were then treated with filtered CM for 6 hours followed by RNA extracted for analysis by RT-qPCR of *GBP2*, *IFIT3* and *IRF7*. Relative gene expression of *GBP2*, *IFIT3* and *IRF7* in BMDMs treated with (G) mtDAMPs (10ug) or (H) CpG ODN 1826. (n=4) Data indicate mean  $\pm$ SD. Statistics are presented as Mann-Whitney U test. \*P < 0.05. (I) BMDM were pre-treated with STING inhibitor H-151 (10 $\mu$ M) for 2 hours before treatment with either CpG ODN 1826 or mtDAMPs (10 $\mu$ g) for 6 hours. RNA was extracted and gene expression was analysed via qRT-PCR. Relative gene expression of *GBP2*, *IFIT3* and *IRF7* in control untreated BMDMs, CpG (n=4). Statistics are presented as two-way ANOVA with Sidak post-hoc multiple comparisons test. \*P < 0.05; \*\*P < 0.01; \*\*\*P < 0.001; \*\*\*\*P < 0.0001.

**Figure 4. MM progression is attenuated by STING Inhibition.** (A) 5TGM1 cells ( $1 \times 10^6$ ) transduced with rLV.EF1.mCherry-Mito9 lentivirus (5TGM1<sup>LUCi+</sup>) were injected KaLwRij mice. (B) In vivo imaging of mice engrafted with 5TGM1<sup>(GFP+ Luci+)</sup> on days 19 and 27, representing before and after H-151 (750 nmol) treatment. (C) Bioluminescence, before and after treatment, was quantified using ImageJ. n=6 in each group. Data indicate mean  $\pm$ SD. Statistics presented as Wilcoxon test \*P < 0.05. (D) Mice were sacrificed at 27 days; BM was harvested for flow cytometry 5TGM1 engraftment (E) and FACS purified for BM macrophages. RNA extracted for analysis by RT-qPCR of *GBP2*, *IFIT3* and *IRF7*. (F) BM cells were analysed for GR1, F4/80, CD115, LY6G, CD11b, CD86, and CD206 expression and used to identify resident BM macrophages (BM M $\Phi$ ) (GR1-, CD115 lo/int, F4/80+) and MM-infiltrating macrophages (IF M $\Phi$ ) (Ly6G-, CD11b+). The gating strategy is shown. (G) Cell counts of (BM M $\Phi$ ) and (IF M $\Phi$ ) from treated mice. Data indicate mean  $\pm$ SD. Statistics presented as Kruskal-Wallis test with Dunn's post-hoc multiple comparisons test. \*P < 0.05; \*\*P < 0.01.

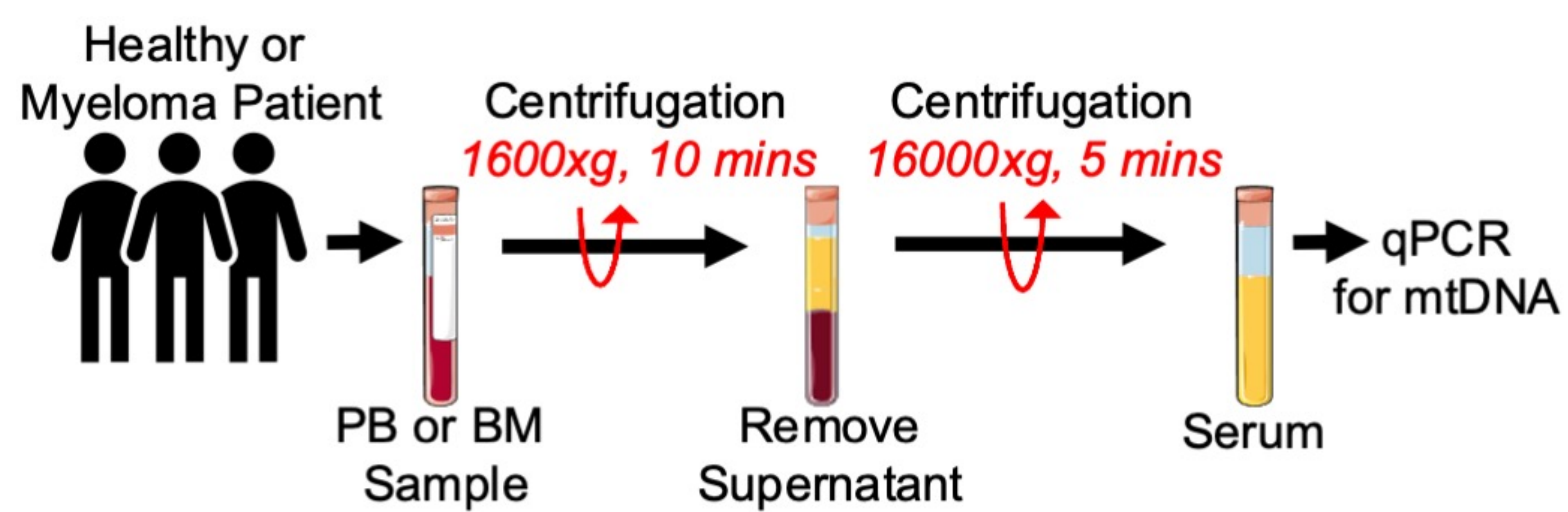
**Figure 5. Myeloma derived mtDAMPs Induce a migratory signature in BM Macrophages.** (A) Schematic of experimental design. BM-derived macrophages

(BMDM) were cultured with mtDAMPs (10µg) for 24 hours. BMDM cell supernatant was cleared of cellular debris by centrifugation prior to cytokine array analysis (n=3)

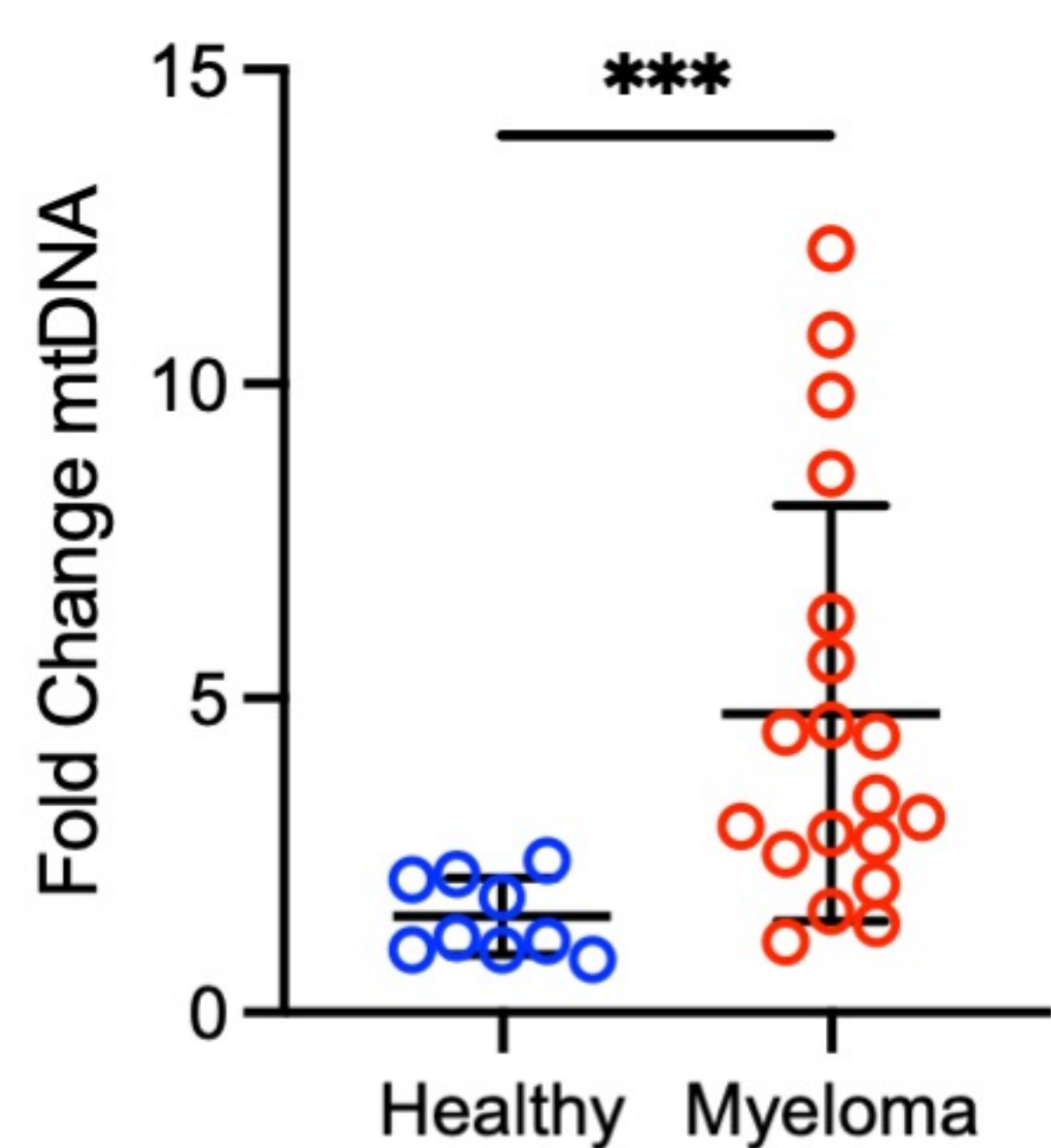
(B) Quantification of cytokine array results segmented into inflammatory and chemoattractant-related factors. (C) Schematic of experimental design. Murine 5TGM1<sup>(GFP+ Luci+)</sup> cells (1x10<sup>6</sup>) were injected into C57BL/KaLwRij mice. On days 20, 22, 24, and 26 post-engraftment, mice were injected intraperitoneally (i.p.) with either 200µl H-151 (750nmol) or vehicle. Mice were sacrificed at 27 days; BM was harvested and myeloma-associated macrophages were isolated via FACS purification. (D) Relative gene expression of *CXCL10*, *CXCL2*, and *CCL5*. n=6 in each treatment group. Data indicate mean ±SD. Statistics presented as Kruskal-Wallis test with Dunn's post-hoc multiple comparisons test. \*P < 0.05; \*P < 0.01. (E) BMDMs were cultured with either mtDAMPs (10µg) alone or mtDAMPs and H-151 (10µM) for 24 hours. BMDM conditioned media was cleared of cellular debris by centrifugation and placed into the bottom chamber of the transwell. 5TGM1<sup>(GFP+)</sup> cells were placed in the upper chamber and migrated 5TGM1<sup>(GFP+)</sup> cells were counted at 4 and 24 hours. Data indicate mean ±SD. Statistics are presented as Mann-Whitney U test. \*P < 0.05. (F) Murine 5TGM1<sup>(GFP+ Luci+)</sup> cells (1x10<sup>6</sup>) were injected into C57BL/KaLwRij mice. At 34 days post-engraftment, peripheral blood (PB) samples were taken by tail vein bleed then mice were injected intraperitoneally (i.p.) with H-151 (750nmol). On day 35, post-treatment blood samples were taken, and mice were sacrificed. The PB samples were analysed for 5TGM1<sup>(GFP+)</sup> cell presence via flow cytometry. n=8 mice. Data indicate mean ±SD. Statistics are presented as Wilcoxon test. \*\*P < 0.01.

Figure 1.

A



B



C

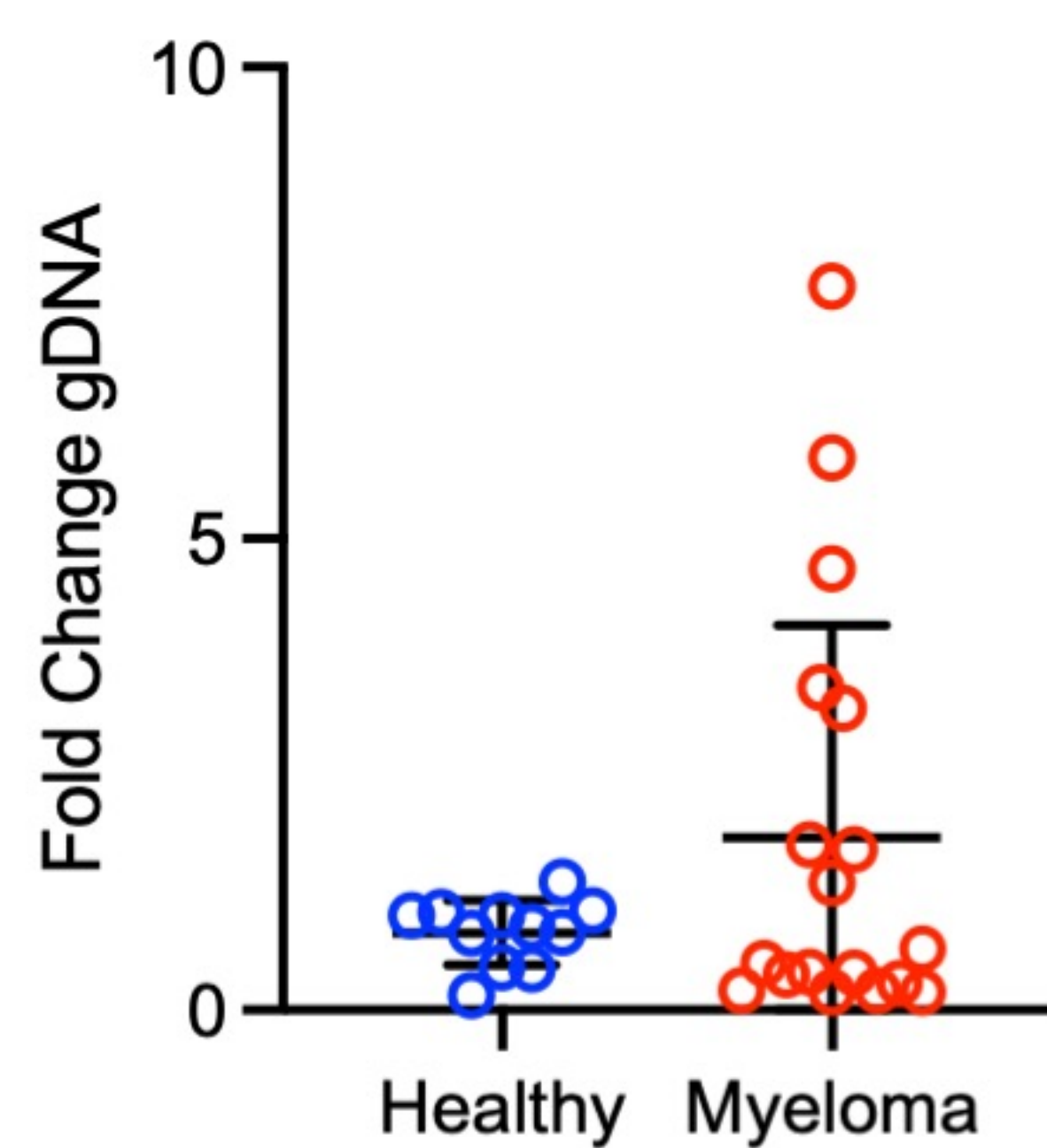


Figure 2.

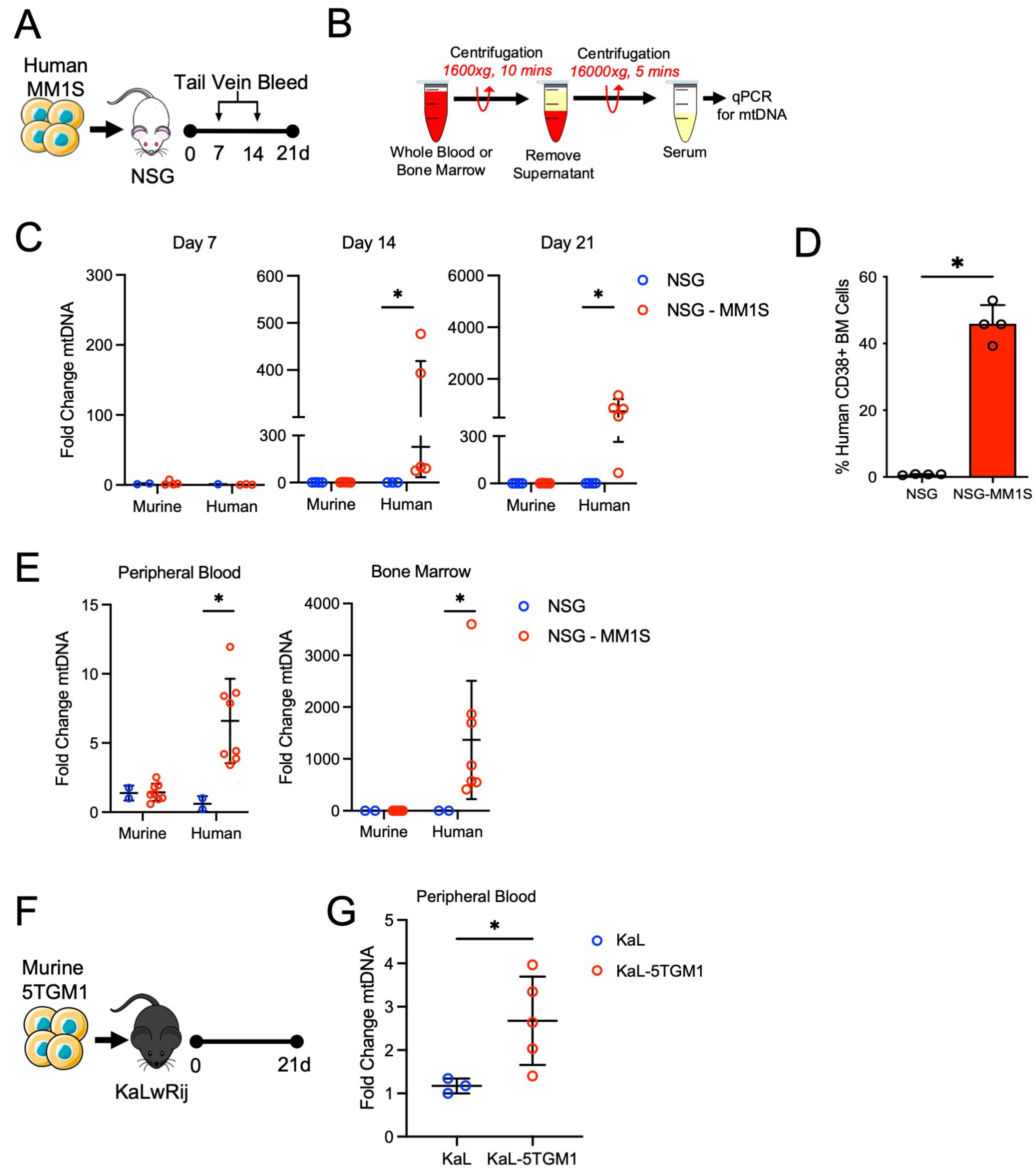


Figure 3.

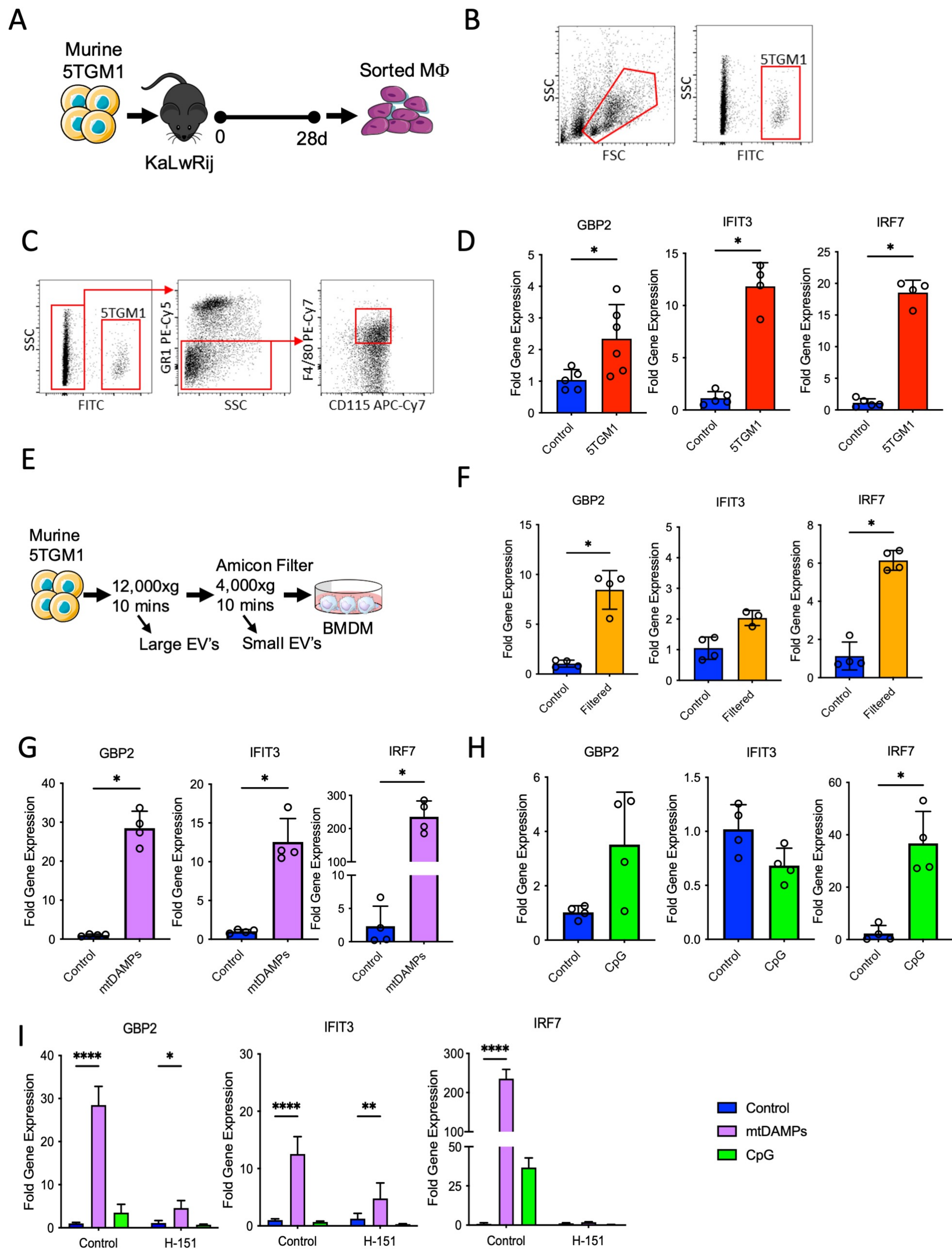
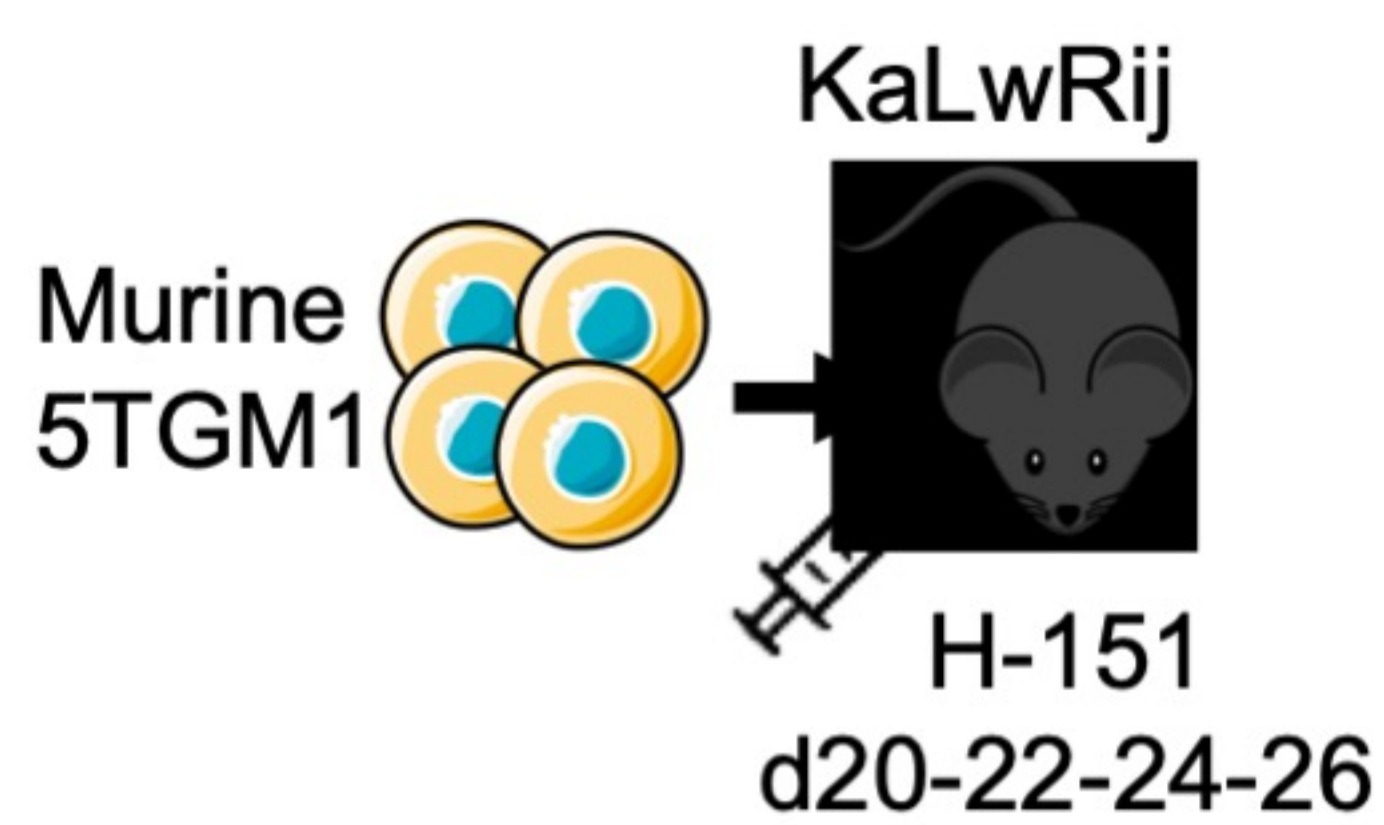
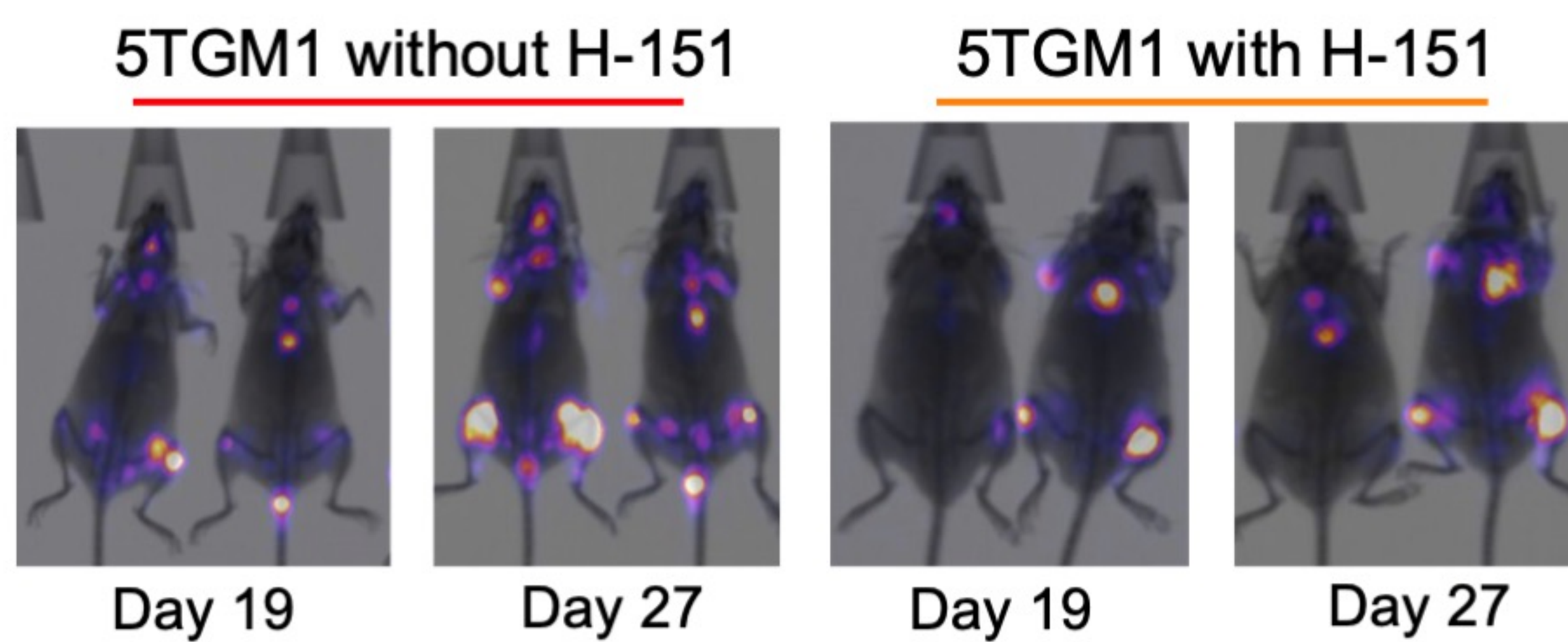


Figure 4.

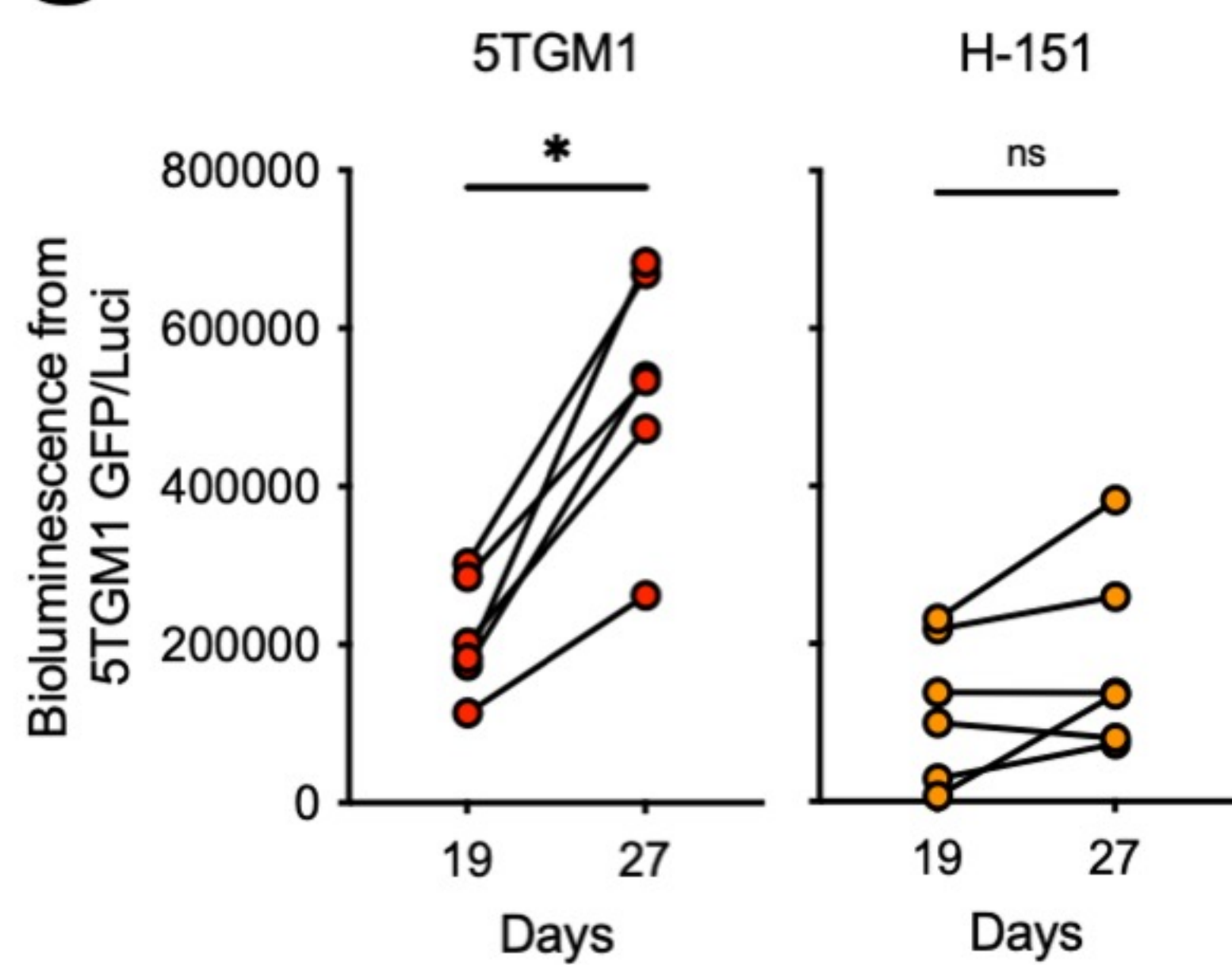
**A**



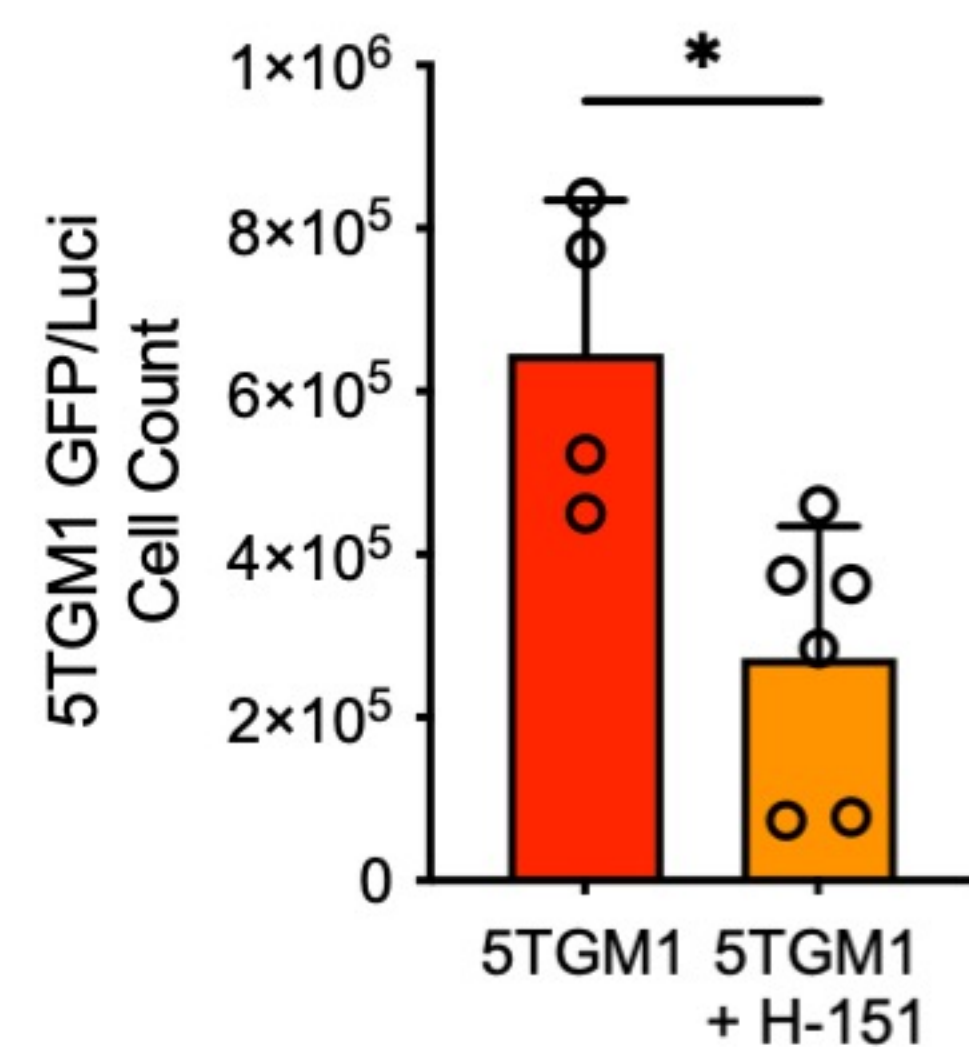
**B**



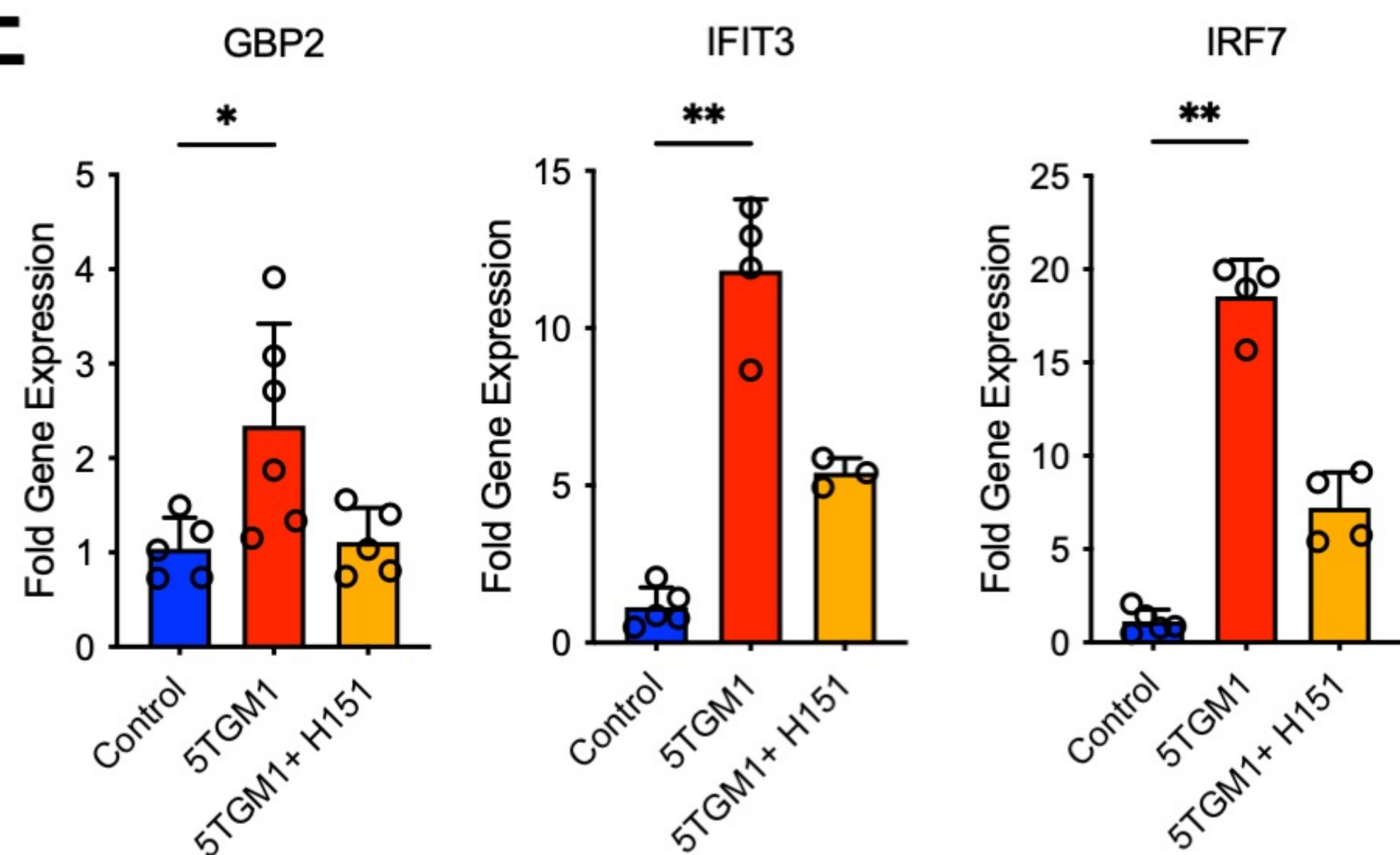
**C**



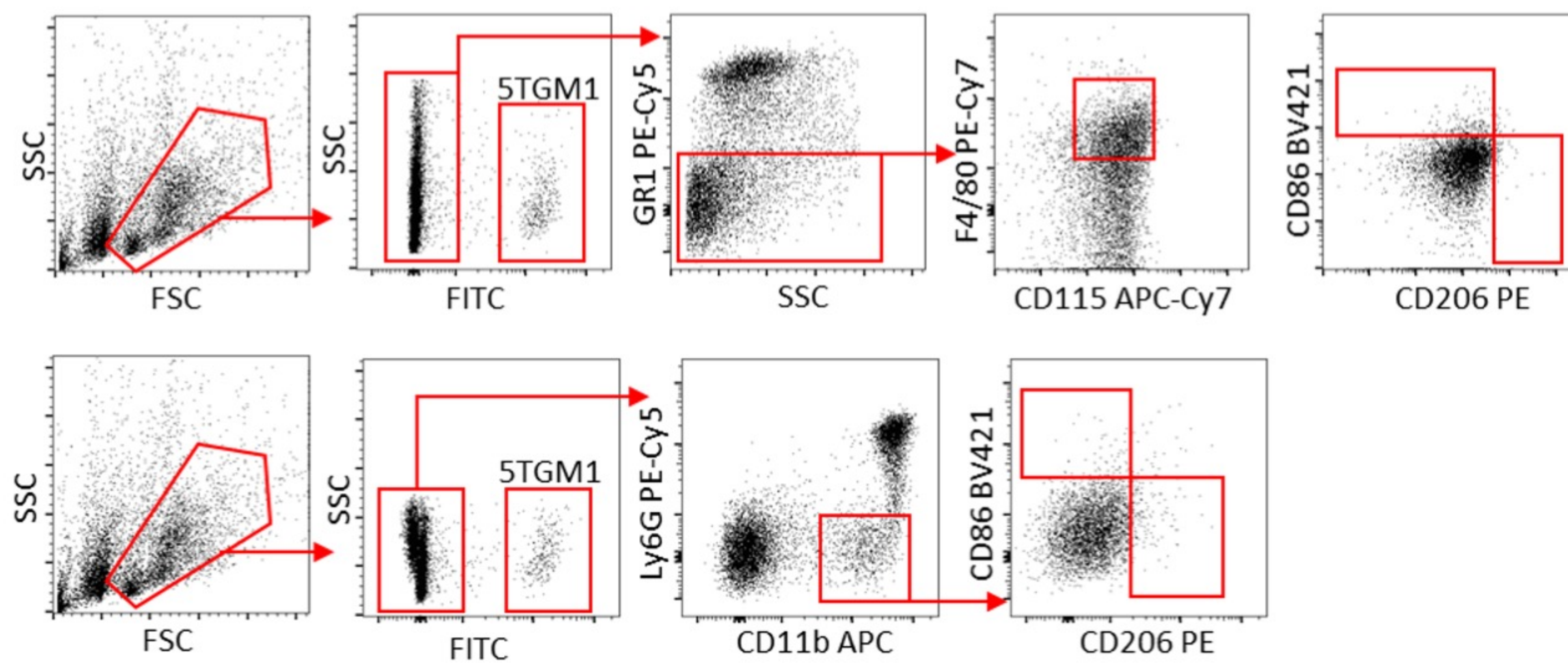
**D**



**E**



**F**



**G**

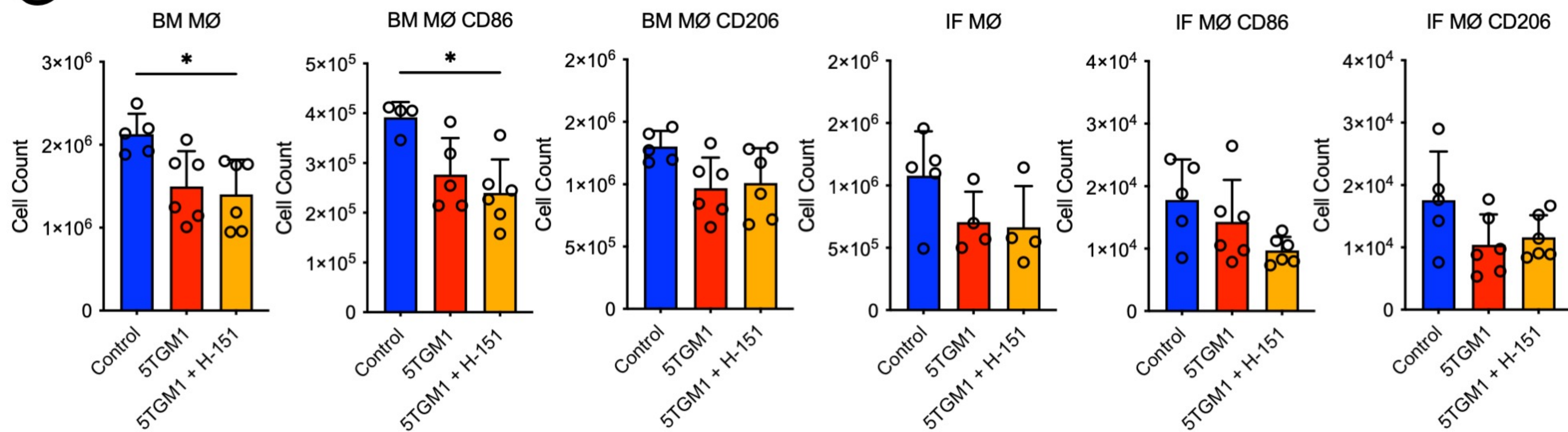
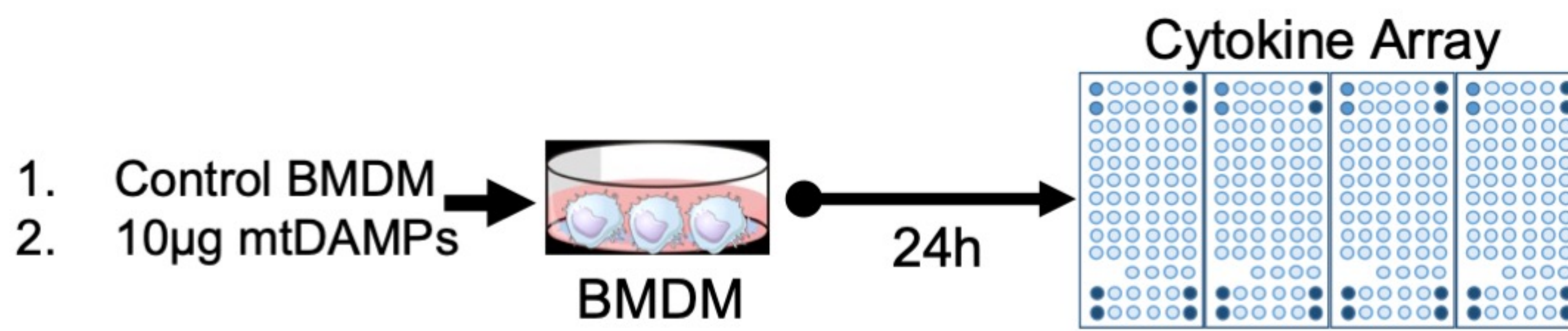
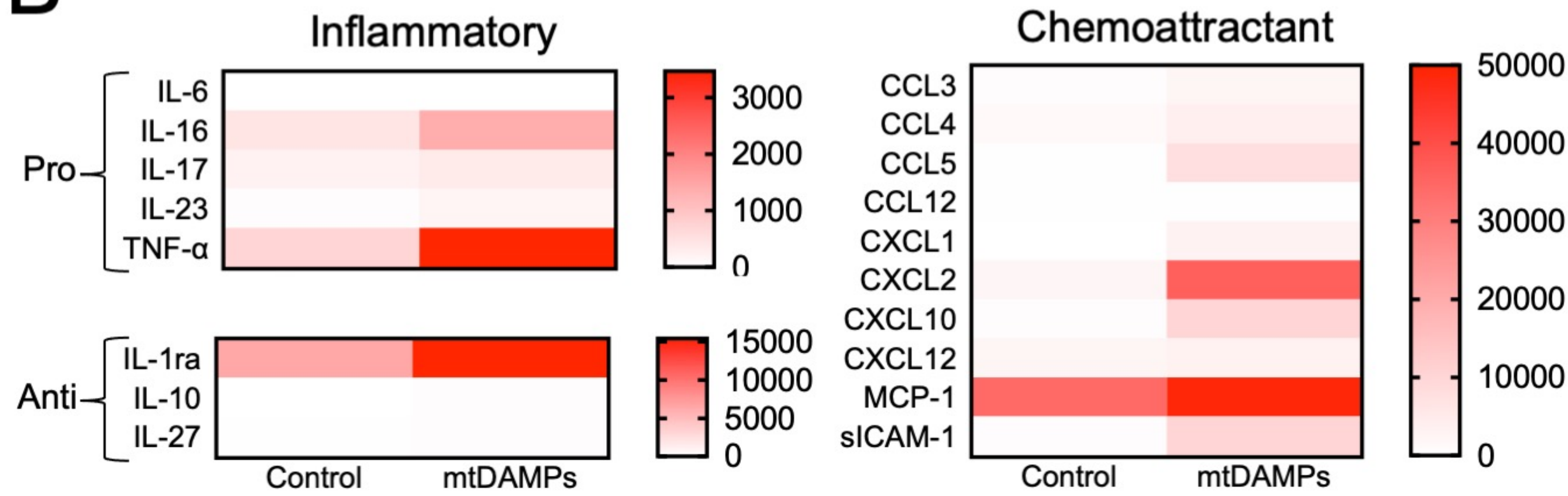


Figure 5.

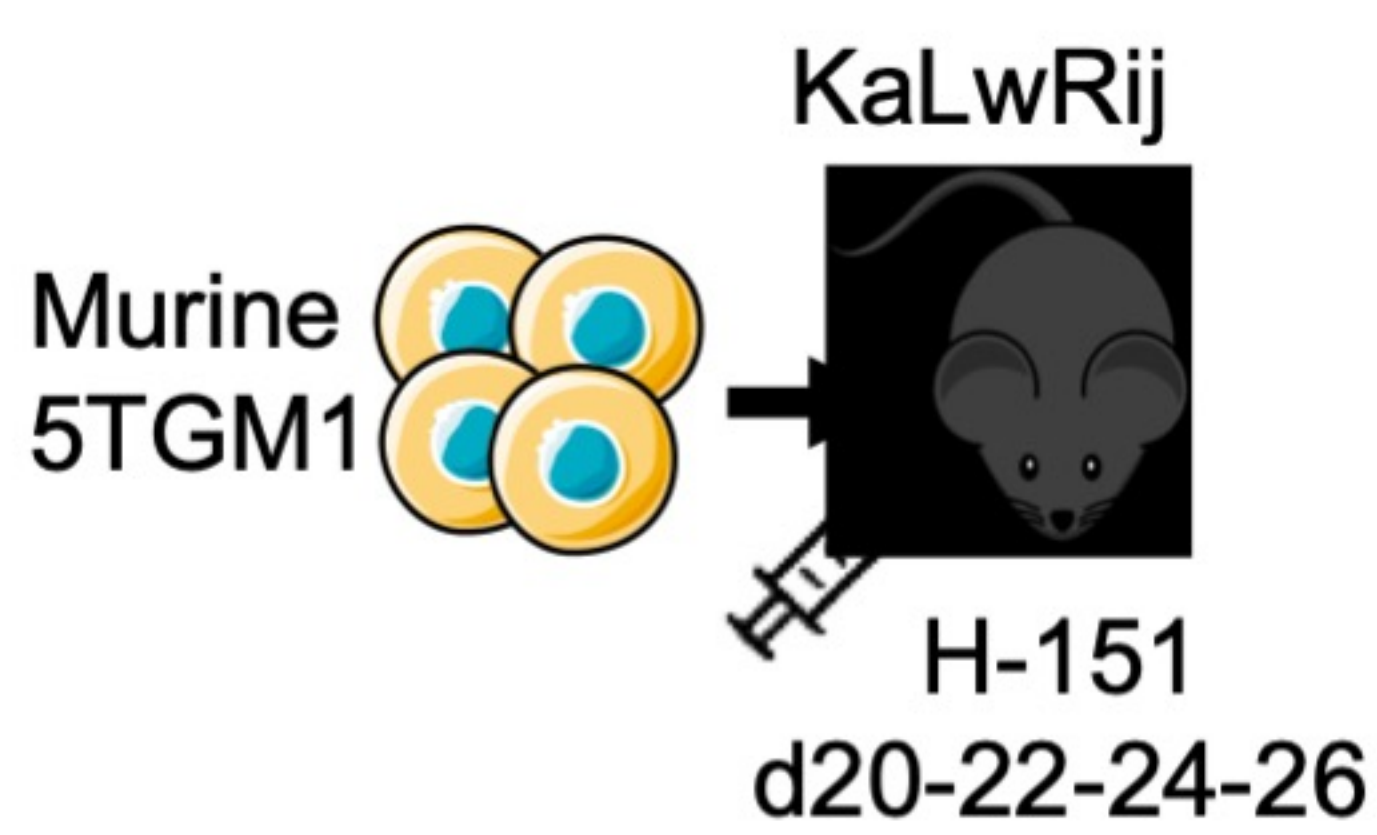
**A**



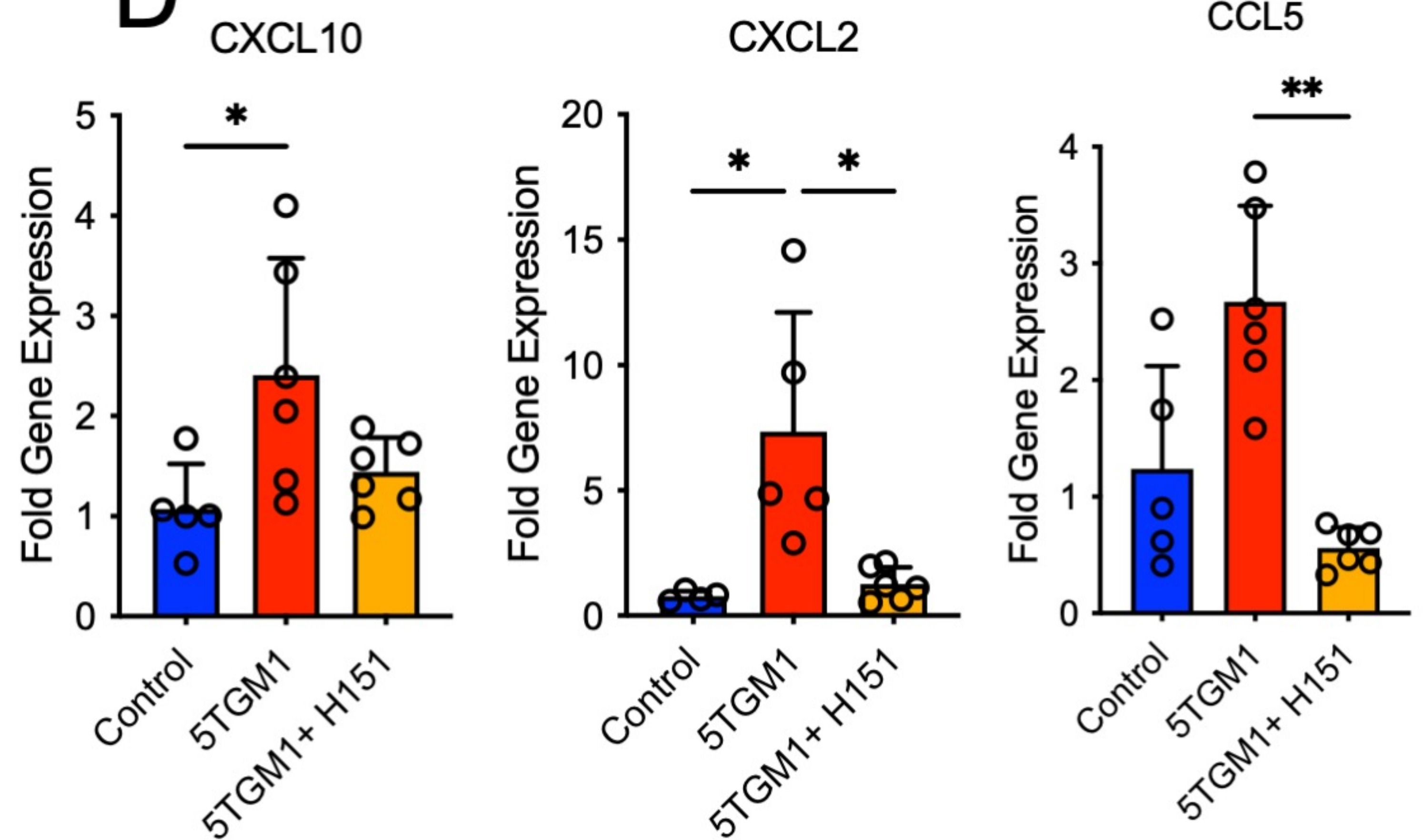
**B**



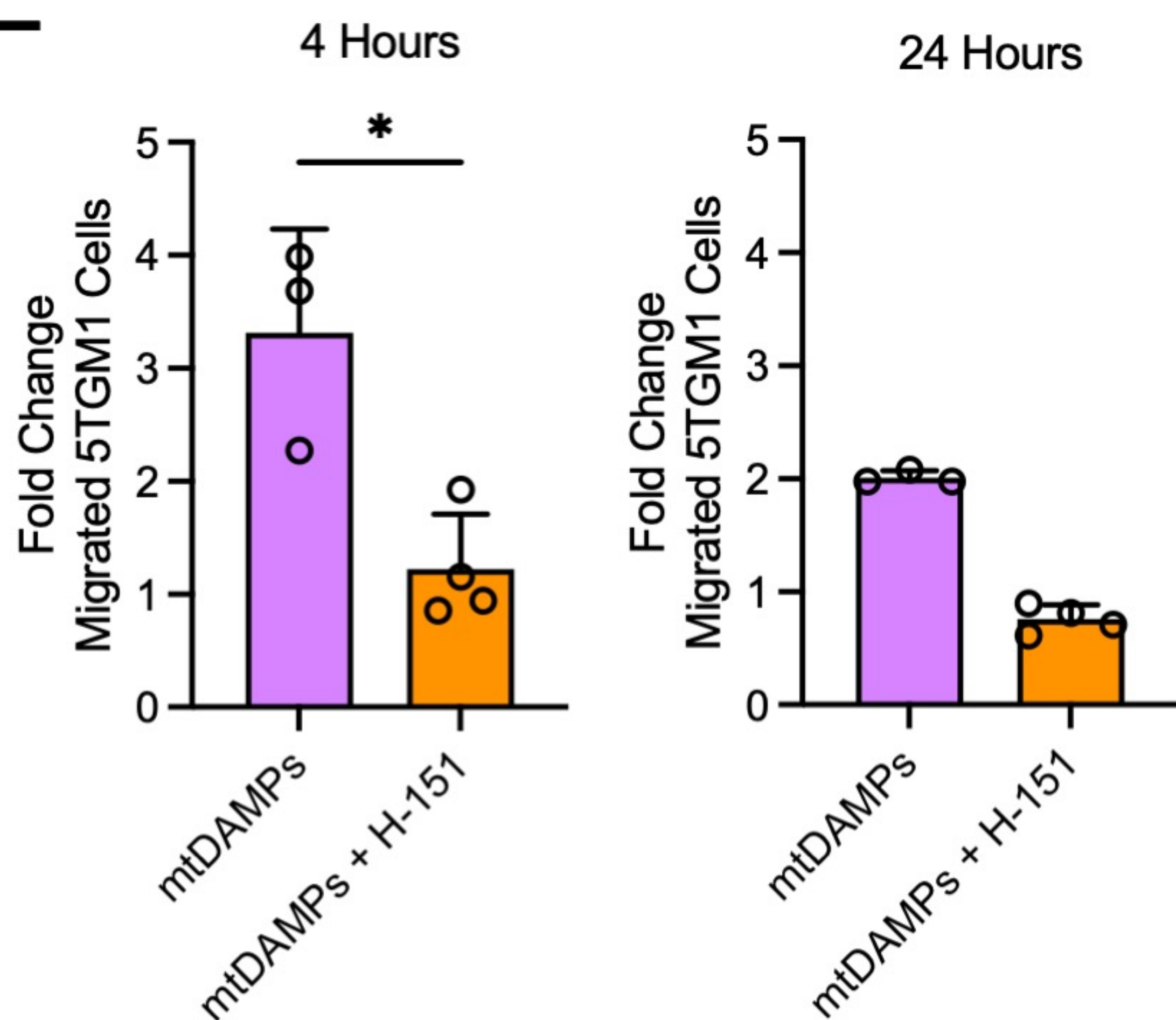
**C**



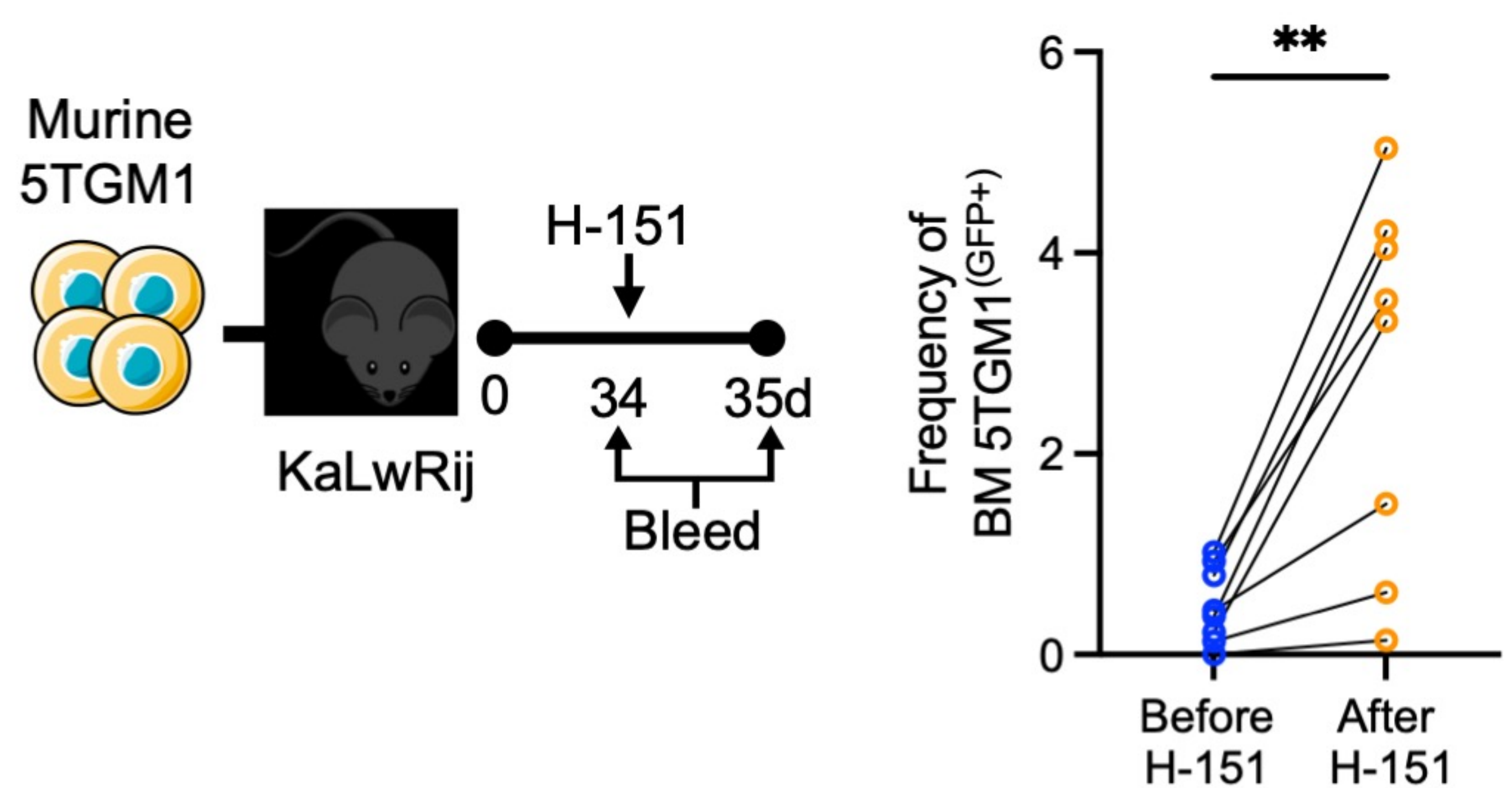
**D**



**E**



**F**



| <b>PATIENT NO.</b> | <b>AGE (YEARS)</b> | <b>SEX</b> | <b>DIAGNOSIS</b> |
|--------------------|--------------------|------------|------------------|
| MM1                | 59                 | F          | Myeloma (s)      |
| MM2                | 74                 | F          | Myeloma (s)      |
| MM3                | 72                 | F          | Myeloma (s)      |
| MM4                | 80                 | M          | Myeloma (a)      |
| MM5                | 37                 | M          | Myeloma (s)      |
| MM6                | 79                 | F          | Myeloma (s)      |
| MM7                | 69                 | M          | Myeloma (a)      |
| MM8                | 57                 | M          | Myeloma (s)      |
| MM9                | 66                 | F          | Myeloma (s)      |
| MM10               | 82                 | F          | Myeloma (a)      |
| MM11               | 74                 | M          | Myeloma (a)      |
| MM12               | 53                 | F          | Myeloma (s)      |
| MM13               | 64                 | M          | Myeloma (s)      |
| MM14               | 73                 | M          | Myeloma (s)      |
| MM15               | 75                 | F          | Myeloma (s)      |
| MM16               | 55                 | M          | Myeloma (s)      |
| MM17               | 75                 | F          | Myeloma (s)      |
| MM18               | 86                 | M          | Myeloma (a)      |
| MM19               | 83                 | F          | Myeloma (a)      |
| MM20               | 72                 | F          | Myeloma (s)      |
| MM21               | 62                 | M          | Myeloma (a)      |
| MM22               | 49                 | F          | Myeloma (a)      |
| MM23               | 80                 | F          | Myeloma (s)      |
| MM24               | 63                 | F          | Myeloma (s)      |
| MM25               | 66                 | F          | Myeloma (a)      |
| MM26               | 60                 | F          | Myeloma (a)      |

F, Female; M, Male; a, Asymptomatic; s, Symptomatic.

Table 1: Myeloma patient data. Samples MM1-MM11 were used for matched analysis of peripheral blood and bone marrow in Figure 1D. Samples MM12-MM19 were used for Figure 1B and C. Samples MM 20-26 were used for Supplementary Figure 2B.